UNIVERSIDADE NOVA DE LISBOA

FACULDADE DE CIÊNCIAS E TECNOLOGIA

Patrícia Carvalho Patrício

Analysis of *PAX2* Gene Alterations in Renal Cell Tumors

Porto

2010

UNIVERSIDADE NOVA DE LISBOA

FACULDADE DE CIÊNCIAS E TECNOLOGIA

Patrícia Carvalho Patrício

Analysis of *PAX2* Gene Alterations in Renal Cell Tumors

Dissertation for applying to a Master's Degree in Molecular Genetics and Biomedicine submitted to the Sciences and Technology Faculty of New University of Lisbon.

Supervisor:
Carmen de Lurdes Fonseca Jerónimo, PhD
(ICBAS – U.Porto, IPO – Porto)

Co-Supervisor:
Rui Manuel Ferreira Henrique, MD, PhD
(ICBAS – U.Porto; IPO – Porto)

Porto

2010

The research project of this master thesis dissertation was developed at the Cancer Epigenetics Group, Department of Genetics and Research Center of the Portuguese Oncology Institute – Porto.

ACKNOWLEDGEMENTS

First of all I wish to thank my supervisor, Prof. Carmen Jerónimo, for giving me the opportunity to work at the Cancer Epigenetics Group, for her guidance, and for all the support and encouragement. Thank you for the valuable advice and for helping me getting started in this world of Science!

I would like to express my gratitude to Prof. Rui Henrique, my co-supervisor, for all the support and pertinent suggestions, and whose great contribution was fundamental for achieving the goals that were proposed.

I am also grateful to Prof. Manuel Teixeira, the Director of the Department of Genetics and Research Center of the IPO Porto, for giving me the privilege to work at his lab.

To Prof. José Paulo Sampaio, the coordinator of this Master Course, and Prof. Nuno Neves, my connection bond to the Faculdade de Ciências e Tecnologia of Universidade Nova de Lisboa, for their assistance and availability during the development and writing process of this thesis.

A special thanks to the members of the Cancer Epigenetics Group, namely Vera, Mafalda, João, Inês and Malini, for your scientific training, helpful suggestions and personal support along this demanding, and sometimes arduous, journey. You undoubtedly gave me the most pleasant work atmosphere I could ever ask for!

My thanks also to Maria, Isabel, Paula, Ricardo, Joana Santos and Joana Guedes for their friendship and support. This work year would not have been the same without our laughs and talks!

Joana Vieira, Diogo and Susana Lisboa, I learned a lot from you and so I could not fail to thank you for your understanding, availability and pertinent suggestions in FISH.

I also want to thank the Department of Anatomic Pathology for their essential contribution for this work, namely to Dr. Ângelo Rodrigues, to Paula Dias and to Isa Carneiro.

I would like to thank the remaining members of the Genetics Department who provided me assistance during this year and whose good mood was always an important motivation in the lab.

Finally, I wish to sincerely thank my parents, my brother and my grandfather, Humberto, and my friends, whose unconditional support was essential at so many stages of my life including this one.

This study was funded by grants from CI-IPOP-4 and the Calouste Gulbenkian Foundation (Project # 96474).

ABBREVIATIONS

AJCC	American Joint Committee on Cancer
BHD	Birt-Hogg-Dubé
BSA	Bovine serum albumine
ccRCC	Clear cell renal cell carcinoma
CD	Collecting duct
cDNA	Complementary DNA
chrRCC	Chromophobe renal cell carcinoma
CpG	Cytosine-phosphate-Guanine
DAPI	4',6-diamidino-2-phenylindole
DCT	Distal convoluted tubule
DEPC	Diethyl pyrocarbonate
DNA	Deoxyribonucleic acid
DNMT	DNA methyltransferase
dNTPs	deoxynucleotides triphosphates
EDTA	Ethylenediamine tetraacetic acid
FFPE	Formalin fixed paraffin embedded
FH	Fumarate hydratase
FISH	Fluorescent *in situ* Hybridization
FLCN	Folliculin
FRET	Förster/ fluorescence resonance energy transfer
GSTP1	Glutathione S-transferase pi 1
HD	Homeodomain
HIF-α	Hypoxia-inducible factor alpha
HPRT1	Hypoxanthine phosphoribosyltransferase 1
IGF2	Insulin-like growth factor 2
MBD	Methyl-CpG-binding domain
miRNA	micro RNA
mRNA	Messenger ribonucleic acid
MSP	Methylation-specific PCR
NaSCN	Sodium thiocyanate

NL	Nephron loop
OP	Octapeptide domain
PAX2	Paired box 2
PBS	Phosphate buffer solution
PCR	Polymerase chain reaction
PCT	Proximal convoluted tubule
PD	Paired-box domain
pRCC	Papillary renal cell carcinoma
qRT-PCR	Quantitative reverse transcription-polymerase chain reaction
RCC	Renal cell carcinoma
RCT	Renal cell tumor
RNA	Ribonucleic acid
SAH	S-adenosylhomocystine
SAM	S-adenosylmethionine
SDS	Sodium dodecyl sulfate
SPSS	Statistical Package for Social Sciences
SSC	Saline-sodium citrate
TD	Transactivation domain
TNM	Tumor-nodes-metastases
TSG	Tumor suppressor gene
UB	Ureteric bud
VHL	Von Hippel-Lindau

SUMMARY

Background: Renal cell tumors (RCT) represent a heterogeneous group of malignancies arising from the epithelium of the renal tubules. *PAX2* (*Paired-box 2*) is a transcription factor belonging to the evolutionarily conserved paired-box family that is required during development of the central nervous system and genitourinary tract. *PAX2*, which is considered a proto-oncogene, is normally suppressed at the later stages of embryonic development and reactivated during the carcinogenic process in some cancer models. Previously published data indicate that significant expression of PAX2 protein occurs in three of the most prevalent renal cell tumor subtypes - clear cell RCC (ccRCC), papillary RCC (pRCC) and oncocytoma - but not in chromophobe RCC (chrRCC). Moreover, it has been reported that *PAX2* expression could be repressed by aberrant methylation at the end of nephrogenesis. Finally, FISH and cytogenetic analysis, demonstrated loss of chromosome 10 (to which *PAX2* is mapped) in 40 to 60% of chrRCC cases.

Aims: The main goal of this study was to identify epigenetic and/or genetic alterations affecting the *PAX2* gene in a series of renal cell tumors, representing the four major subtypes. Specifically, our aims were to: (1) analyze the expression of *PAX2* in different renal cell tumor subtypes, both at mRNA and at protein level; (2) determine whether the regulation of *PAX2* expression occurs by epigenetic mechanisms, by assessing its promoter methylation status; (3) analyze the association between *PAX2* copy number and gene expression; (4) evaluate the potential use of *PAX2* epigenetic/genetic alterations as a biomarker for discrimination between chrRCC and oncocytoma.

Methodology: In this study, 120 samples of renal cell tumors (30 of each subtype: ccRCC, pRCC, chrRCC, and oncocytoma) and 4 normal kidney tissues were tested. First, PAX2 protein expression was assessed by immunohistochemistry and the *PAX2* mRNA expression levels were determined by quantitative reverse transcription PCR (qRT-PCR), using *HPRT1* as an endogenous control. The methylation status of *PAX2* promoter was assessed by methylation-specific PCR using two different sets of primers that annealed to adjacent regions in the promoter. The relationship between the number of *PAX2* copies and its expression in chrRCC was analyzed by FISH.

The chi-square test or Fisher's exact test were used to seek for differences in the frequency of immunoreactivity for PAX2 protein among the four RCT subtypes.

Differences in *PAX2* mRNA expression levels among the four groups were assessed by the Kruskal-Wallis non-parametric test, followed by pairwise comparisons using the Mann-Whitney U test, when appropriate. The relationship between FISH findings and immunoexpression results for chrRCC was assessed by a chi-square or Fisher's exact test, and the directional measure Somers'd was also computed. Moreover, the association between FISH findings and *PAX2* mRNA levels for chrRCC was estimated using the Kruskal-Wallis test.

Results and Discussion: Immunohistochemical results showed high immunoexpression score (> 10% positive cells) for ccRCC (96.7%), oncocytoma (90%) and pRCC (56.6%), whereas chrRCC had low immunoexpression score (33.3%), and these differences reached statistical significance ($p < 0.001$).

Concerning *PAX2* mRNA expression, significant differences among the renal cell tumor subtypes ($p < 0.001$) were detected. Although *PAX2* mRNA expression levels did not differ between ccRCC and pRCC, both were significantly higher when compared to chrRCC and oncocytoma ($p < 0.001$, except for papillary *vs.* oncocytoma: $p = 0.011$). Moreover, mRNA expression levels in renal oncocytomas also differed significantly from those of chrRCC ($p < 0.001$). Finally, transcript levels correlated with the immunoexpression results.

No methylation was found in the renal cell tumor tissues or in the normal kidney tissues, using the two different sets of primers, excluding this epigenetic alteration as a putative mechanism for *PAX2* downregulation in renal cell tumors.

FISH analyses showed that 69% of chrRCC presented chromosome 10 monosomy, correlating with PAX2 immunoexpression and, thus, suggesting that this alteration might be responsible for low *PAX2* expression. The remaining chrRCC cases had no chromosome 10/*PAX2* copy number changes (23%) or displayed three to four copies (8%). However, no correlation was observed between chromosome 10/*PAX2* copy number changes and mRNA expression levels, although, a positive trend was suggested.

Conclusions: Although the PAX2 immunoexpression results in this study diverge slightly from those previously published, our findings confirm that it might be useful as an ancillary tool for the distinction between chrRCC and renal oncocytoma.

This study was the first to determine *PAX2* mRNA expression levels for the four most representative renal cell tumor subtypes, and these results were found to correlate with protein immunoexpression.

Importantly, we also demonstrated that *PAX2* promoter methylation is not involved in *PAX2* silencing in chrRCC. Indeed, FISH analysis showed that *PAX2* downregulation in this tumor subtype is likely due to chromosome 10 monosomy.

RESUMO

Introdução: Os tumores de células renais representam um grupo heterogéneo de tumores com origem no epitélio dos túbulos renais. O gene *PAX2* (*Paired-box 2*) é um factor de transcrição da família *Paired-box*, conservada em termos evolutivos, sendo necessário durante o desenvolvimento do sistema nervoso central e genito-urinário. Este gene, considerado um proto-oncogene, é normalmente silenciado nos estadios finais do desenvolvimento embrionário e reactivado durante o processo carcinogénico em alguns modelos de cancro. Dados publicados anteriormente indicam que ocorre imuno-expressão significativa do PAX2 em três dos subtipos de tumores de células renais mais prevalentes – carcinoma de células renais de células claras (ccRCC), carcinoma de células renais papilar (pRCC) e oncocitoma – mas não no carcinoma de células renais cromófobo (chrRCC). Foi ainda descrito que a expressão do gene *PAX2* poderia ser silenciada por metilação aberrante do promotor no final da nefrogénese. Finalmente, análises citogenéticas demonstraram que a perda do cromossoma 10 (no qual o *PAX2* está localizado) ocorre em 40 a 60% dos casos de chrRCC.

Objectivos: O principal objectivo deste estudo foi identificar alterações genéticas e/ou epigenéticas do gene *PAX2* numa série de tumores de células renais representativa dos quatro subtipos mais prevalentes. Especificamente, os nossos objectivos foram: (1) analisar a expressão do gene *PAX2* em diferentes subtipos de tumores de células renais, tanto ao nível do transcrito (mRNA) como ao nível da proteína; (2) determinar se a regulação da expressão do gene *PAX2* ocorre por mecanismos epigenéticos, analisando o estado de metilação do seu promotor; (3) analisar a relação entre o número de cópias do gene *PAX2* e a sua expressão; (4) avaliar o potencial uso das alterações genéticas/epigenéticas do gene *PAX2* como biomarcadores para a discriminação entre chrRCC e oncocitoma.

Metodologia: Neste estudo foram testadas 120 amostras de tumores de células renais (30 amostras de cada subtipo: ccRCC, pRCC, chrRCC e oncocitoma) e 4 amostras de tecido de rim normal. Inicialmente, foi determinada a expressão da proteína por imuno-histoquímica e os níveis de expressão do transcrito do gene *PAX2* por PCR quantitativo de transcriptase reversa, usando o gene *HPRT1* como controlo endógeno. O estado de metilação do promotor do gene *PAX2* foi analisado através de PCR específico para metilação utilizando dois conjuntos diferentes de *primers* que hibridam em regiões

adjacentes no promotor. A relação entre o número de cópias do gene *PAX2* e a sua expressão nos chrRCC foi analisada por hibridação fluorescente *in situ* (FISH).

O teste de Qui-quadrado foi utilizado para pesquisar diferenças nas frequências de imunorreactividade para a proteína PAX2 entre os quatro subtipos de tumor de células renais. Para avaliar as diferenças nos níveis de expressão de transcrito entre os quatro grupos de tumores procedeu-se a um teste não-paramétrico de Kruskal-Wallis, seguido de comparações emparelhadas usando o teste U Mann-Whitney. A relação entre os resultados de FISH e de imunoexpressão foi determinada utilizando o teste de Qui-quadrado e o teste de Somers'd. Adicionalmente, a associação entre os resultados de FISH e os níveis de expressão de transcrito foi estimada utilizando um teste de Kruskal-Wallis.

Resultados e discussão: Os resultados da análise imuno-histoquímica revelaram elevada frequência de imunorreactividade (mais de 10% de células positivas) em ccRCC (96,7%), oncocitoma (90%) e pRCC (56,6%), enquanto que o chrRCC apresentou uma baixa frequência de imunorreactividade (33,3%), sendo estas diferenças estatisticamente significativas ($p < 0,001$).

Relativamente à expressão do transcrito do gene *PAX2*, foram detectadas diferenças significativas entre os diferentes subtipos de tumores de células renais ($p < 0,001$). Apesar de não terem sido detectadas diferenças nos níveis de transcrito entre ccRCC e pRCC, ambos apresentaram níveis significativamente mais elevados quando comparados com chrRCC e oncocitoma ($p < 0,001$ excepto no caso de pRCC *vs*. oncocitoma: $p = 0,011$). Além disso, os níveis de expressão de transcrito nos oncocitomas também diferiram dos encontrados para chrRCC ($p < 0,001$). Os níveis de transcrito correlacionaram-se significativamente com os resultados de imuno-histoquímica.

Não foi identificada metilação do promotor do PAX2 tanto nos tumores de células renais como no tecido renal normal, usando ambos os conjuntos de *primers*. Assim, esta alteração epigenética ficou excluída como mecanismo responsável pela sub-expressão do gene *PAX2* em tumores de células renais.

A análise de FISH revelou que 69% dos casos de chrRCC apresentava monossomia do cromossoma 10, correlacionando-se com a imuno-expressão, sugerindo que esta alteração deverá ser responsável pela sub-expressão do gene *PAX2*. Os restantes casos de chrRCC não apresentaram alterações do número de cópias do cromossoma 10/gene *PAX2* (23%) ou apresentaram três ou quatro cópias (8%). Contudo, não foi verificada correlação

entre o número de cópias do cromossoma 10/gene *PAX2* e os níveis de expressão de transcrito, apesar da aparente tendência de associação entre os dois parâmetros.

Conclusões: Apesar de os resultados de imuno-histoquímica para o gene *PAX2* neste estudo divergirem ligeiramente dos previamente publicados, eles confirmam que esta pode ser útil como ferramenta auxiliar para a distinção entre chrRCC e oncocitoma.

Este estudo foi o primeiro a determinar os níveis de expressão de transcrito do gene *PAX2* nos quatro subtipos de tumores de células renais mais representativos e estes resultados mostraram estar correlacionados com a imuno-expressão.

Também demonstramos que a metilação do promotor do gene *PAX2* não está envolvida no silenciamento deste gene nos chrRCC. De facto, a análise de FISH indica que a sub-expressão do gene *PAX2* neste subtipo de tumor se deverá à monossomia do cromossoma 10.

INTRODUCTION

1. Anatomy and Histology of the Kidney

The urinary system consists of six organs: two kidneys, two ureters, the urinary bladder, and the urethra (Saladin, 2001).

The most fundamental roles of the kidneys are homeostatic balance of the volume and composition of the body fluids, such as the blood plasma, tissue fluid, and intracellular fluid, the removal of waste products from the blood, and the regulation of the blood pressure by secreting several hormones (Chow *et al.*, 2010).

Each kidney is composed of a parenchyma and a collecting system. The parenchyma includes an outer cortex and an inner medulla, and is composed of about 1.2 million functional units, the nephrons. Each nephron consists of three principal parts: the blood vessels, the renal corpuscle, and a long renal tubule.

The renal corpuscle consists of a glomerulus enclosed in a two-layered glomerular (Bowman's) capsule. The fluid that filters from the glomerular capillaries is called the glomerular filtrate.

The renal tubule is a duct that leads away from the glomerular capsule and is divided into four major regions: the proximal convoluted tubule (PCT), the nephron loop (loop of Henle, NL), the distal convoluted tubule (DCT), and the collecting duct (CD). Each region has specific physiological functions in the production of urine. The PCT arises from the glomerular capsule and is the longest of the four regions, dominating the histological sections of renal cortex, and is where most of the absorption occurs. The following region is the loop of Henle, a long U-shaped structure which is divided into the thick and the thin segments. The thick segment cells are engaged in the active transport of salts, and have a very high metabolic activity as it is reflected by its large amount of mitochondria. The thin segment cells have low metabolic activity but are very permeable to water (Saladin, 2001).

The DCT is shorter and less convoluted than PCT, and so fewer sections are seen in histological sections. This region determines the end of the nephron.

Finally, the collecting duct consists of the region to which several nephrons drain into (Saladin, 2001).

The nephrons are supported by a mesenchyme composed by interstitial cells interspersed with extracellular matrix elements, nerves and vessels. Interstitial cells may be

divided in renal fibroblasts and cells of the immune system, and are engaged in the modeling of the extracellular matrix, in the production of regulatory substances, including erythropoietin, and in immune processes (Lemley and Kriz, 1991).

2. Kidney Cancer

2.1 Epidemiology

Cancer is currently the second major cause of death in Western World countries, and kidney cancer accounts for approximately 4% of all cancers, being the 7th most common cancer in men and the 8th most common in women (Jemal *et al.*, 2010).

In 2008, approximately 167,947 new cases of kidney cancer were diagnosed and 72,030 persons died because of this malignancy, worldwide (Ferlay *et al.*, 2010b).

In Europe, the estimated number of kidney cancer cases and deaths in 2008 was 88,400 and 39,300, respectively, for both sexes. In Portugal, the estimated incidence of kidney cancer cases in 2008 was 4.3 and 2.5 hundreds, for males and females, respectively (Ferlay *et al.*, 2010a). Mortality to incidence ratio in kidney cancer is higher compared to other urological malignancies (Lindblad, 2004).

Adult kidney cancers arising in the renal parenchyma are mainly adenocarcinomas, also known as renal cell carcinomas (RCC). Those arising from the collecting system are mainly transitional cell carcinomas (Chow *et al.*, 2010). Renal cell carcinomas represent more than 90% of all renal malignancies occurring in adults in both sexes being the 12th most common cancer in men and the 17th in women (Eble *et al.*, 2004).

The incidence of RCC varies considerably worldwide. The highest incidence rates are registered in Europe, North America and Australia, while the lowest occur in Asia, South America and Africa (Figure 1) (Ferlay *et al.*, 2010b).

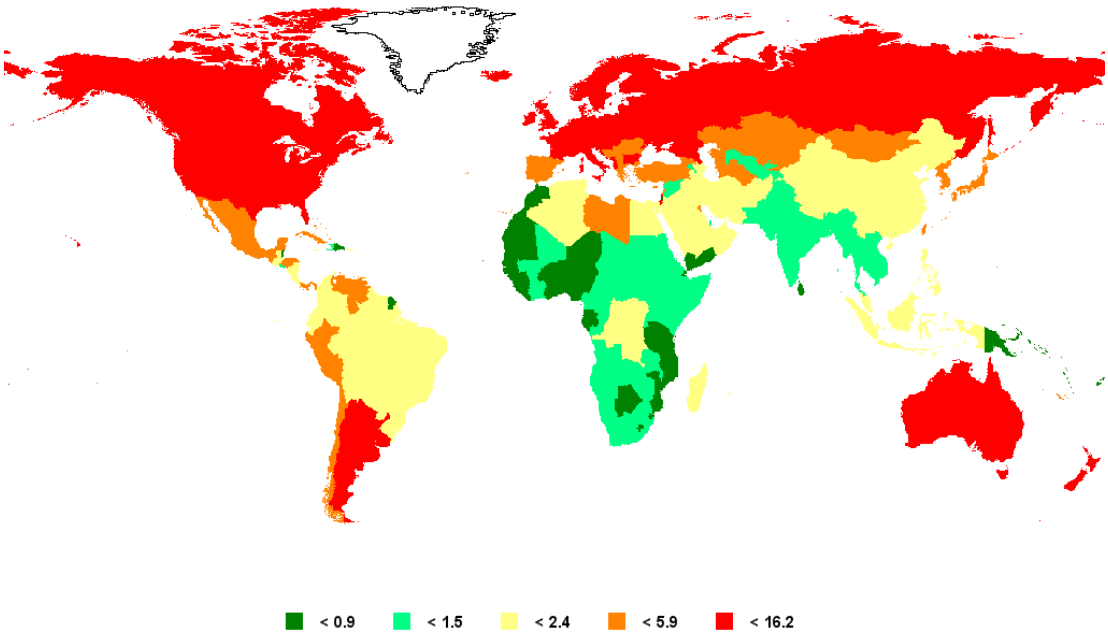

Figure 1: Worldwide distribution of kidney cancer incidence. In 2008, the highest incidence rates for this malignancy, for both genders, were registered in Europe, North America and Australia.

Adapted from IARC, GLOBOCAN, 2008 (Ferlay et al., 2010b).

The incidence rates for this carcinoma have been rising each year in some developed countries. This fact cannot be explained completely by the use of imaging techniques, which improves early detection of small size tumors, but also by the increasing etiologic risk factors prevalence and exposure (Lindblad, 2004).

2.2 Risk factors

Renal Cell Carcinoma etiology is difficult to address. However, some risk factors have been consistently reported to be positively associated with this malignancy.

Gender, age, ethnicity, cigarette smoking, obesity, dialysis treatment, hypertension and use of antihypertensive medication are some of those risk factors already reported.

2.2.1 Gender, Age and Ethnicity

Renal cell carcinoma is more frequent in men than in women, with a men to women ratio of 3/2 (Lindblad, 2004).

Older individuals are at higher risk compared with young individuals. In fact, the peak incidence occurs in the sixth decade, with the majority of the cases (80%) occurring within 40 to 69-year-old population (Pascual and Borque, 2008).

Kidney cancer incidence is 10 to 20% higher in african-americans although the reason is not completely understood (Chow *et al.*, 1999).

2.2.2 Cigarette smoking

This is one of the most well established risk factors for RCC and is thougth to account for approximatly 39% of all cases in males. However, increased risk has most often been found in long-term or heavy smokers (Muscat, 2000).

The two major classes of tobacco carcinogens are the polycyclic aromatic hydrocarbons (PAH) such as benzo[a]pyrene and the tobacco-specific nitrosamines. Most of these tobacco smoke constituents are metabolized or excreted. Although it is not clear which of these constituents are responsible for RCC, some studies reported that nitrosamines could induce renal tumors in several animal species (Muscat, 2000).

2.2.3 Dialysis

Approximately 45% percent of dialysis patients develop acquired cystic disease of the kidney. These patients show a 30 times higher risk for developing RCC than the rest of the general population (Pascual and Borque, 2008; Anglada Curado *et al.*, 2009).

2.2.4 Hypertension and antihypertensive medication

Hypertension and the use of antihypertensive medication have been reported to be risk factors for RCC in several epidemiological studies. It is unclear, however, whether the increased risk is caused by hypertension itself, or by the use of antihypertensive medication. The mechanisms contributing to this increased risk are not totally understood but it seems that the consequent metabolic and/or functional changes in the renal tubular cells may underlie the onset of carcinogenesis (Pascual and Borque, 2008).

2.2.5 Obesity

Several epidemiological studies correlate hypercaloric diet and obesity with an increased risk for developing RCC. The mechanism by which obesity causes kidney cancer is not very clear, but it has been hypothesized that it may be due to secondary hormonal

changes, decreased immune system, or associated hypertension and/or diabetes mellitus (Pascual and Borque, 2008; Lowrance *et al.*, 2010). Although this is a very discussed putative risk factor, direct evidence for these mechanisms in humans is limited.

2.2.6 Inheritance

Although most of the cases of RCC are sporadic, approximately 4% of the Renal Cell Carcinomas are associated with hereditary syndromes. The presence of multiple neoplastic renal lesions or family history suggest genetic predisposition to this disease (Anglada Curado *et al.*, 2009).

There are four major hereditary syndromes that predispose to RCC: The Von Hippel-Lindau syndrome, hereditary leiomyomatosis and renal cell carcinoma, Birt-Hogg-Dubé syndrome and hereditary papillary RCC.

Von Hippel-Lindau (VHL) syndrome:

This syndrome is caused by germline mutations of the *VHL* tumor suppressor gene, located on chromosome 3p25-26. Heritable clear cell RCC is caused by a germline mutation of one allele and an acquired mutation of the second allele. These germline mutations are identified in nearly 100% of *VHL*-families (Baldewijns *et al.*, 2008). The VHL protein has an important role in cell cycle regulation and angiogenesis (Maxwell *et al.*, 1999).

Clinical manifestations include, among others, the risk for development of RCC, pheochromocytoma, pancreatic cysts and retinal angiomas. The RCC is of the clear cell type and may be solid or cystic (Rosner *et al.*, 2009). Fourty to sixty percent of the patients with this syndrome present a RCC (Pascual and Borque, 2008).

Hereditary papillary renal cell carcinoma:

This is an inherited tumor syndrome with autosomal dominant trait and of late onset, with multiple bilateral papillary RCCs type I. The disease is caused by activating mutations of the *MET* proto-oncogene which maps the chromosome 7q31.1 (Pascual and Borque, 2008). Trisomy of chromosomes 7 and 17 are typical of these tumors, which is also common in the sporadic papillary RCC (Lopez-Beltran *et al.*, 2009).

Hereditary leiomyomatosis and renal cell carcinoma:

This is an autosomal dominant tumor syndrome characterized by germline mutations in the fumarate hydratase (*FH*) gene, located in the chromosome 1q42.3–q43. Mutations in this gene can produce an overexpression of hypoxia inducible factors HIF-1α and HIF-2α leading to the activation of several hypoxia-inducible gene targets (Algaba, 2010). Patients who have this syndrome have the tendency to acquire cutaneous and uterine leiomyomas, and occasionally papillary renal cell carcinoma type II and uterine leiomyosarcomas (Pascual and Borque, 2008). Loss of heterozygosity at 1q32 and 1q42-44 is frequently found. These tumors usually have poor prognosis and frequently spread to regional lymph nodes (Lopez-Beltran *et al.*, 2009).

Birt-Hogg-Dubé syndrome:

This is a hereditary cancer syndrome with an autosomal dominant inheritance pattern as well. It is characterized by benign skin tumors and multiple renal tumors, such as chromophobe RCC (33%), hybrid tumors (50%) and oncocytoma (35%). Clear cell RCC has also been identified in several cases (Pascual and Borque, 2008; Rosner *et al.*, 2009).

The gene associated with this syndrome, known as *FLCN* or *BHD* that maps to the chromosome 17p11.2*,* encodes a protein called folliculin which is truncated as a result of insertions, deletions, or nonsense mutations. This is a characteristic tumor suppressor gene and is also involved in sporadic RCC (Pascual and Borque, 2008; Rosner *et al.*, 2009).

3. Pathology and Classification

Renal cell tumors (RCT) represent a heterogeneous group of neoplasms arising from the epithelium of the renal tubules. Histological and molecular evaluation of this group of tumors has resulted in the development of a universal classification consisting of several different RCT subtypes (Baldewijns *et al.*, 2008). The Heidelberg classification of RCT emerged in 1996, and integrates data from recognizable histological criteria and genetic changes (Kovacs *et al.*, 1997). A diagram representing this classification system is shown in Figure 2.

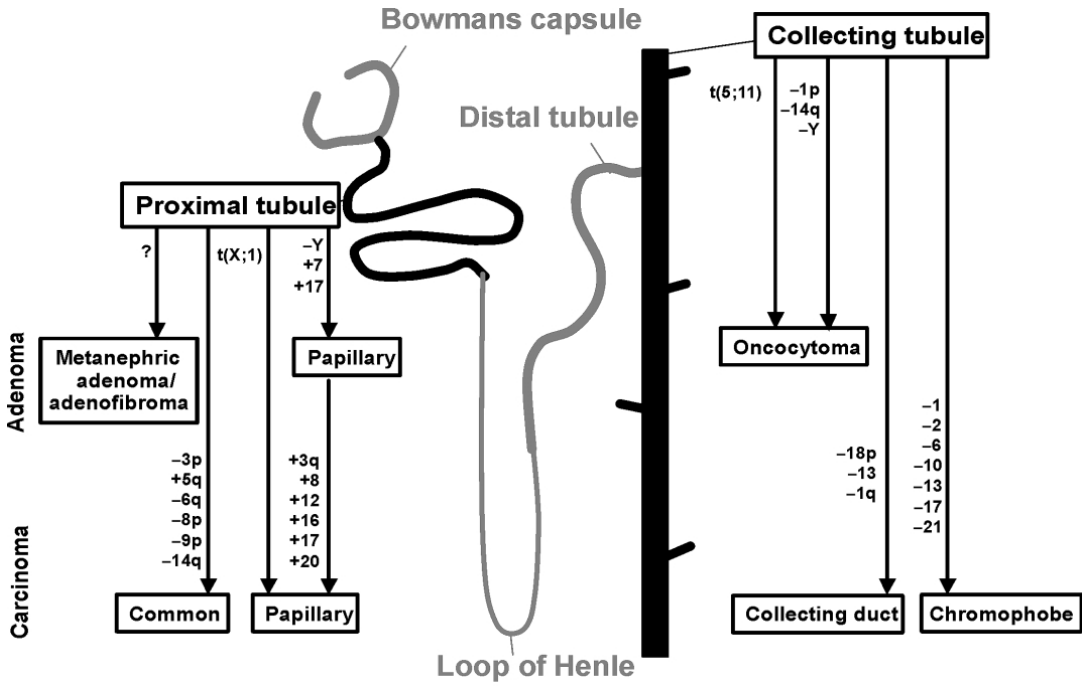

Figure 2: Diagram representing the different subtypes of RCC according to the "Heidelberg" classification. Localization of the subtypes and cytogenetic changes associated to each subtype.

Adapted from (Bodmer et al., 2002).

This classification separates benign from malignant epithelial neoplasms. It comprises three major histological subtypes of renal cell carcinoma (RCC): clear cell RCC, papillary RCC and chromophobe RCC. Collecting duct RCC is a fourth, less common, subtype of malignant renal tumor. Other rare variants are also recognized. Benign tumors have been subclassified into metanephric adenoma/adenofibroma, papillary renal cell adenoma and renal oncocytoma, the most common of these (Bodmer *et al.*, 2002).

3.1 Clear cell Renal Cell Carcinoma

Clear cell RCC (ccRCC) or common RCC is the most frequent subtype of RCC. It comprises more than 70% of all RCCs and is thought to arise from the proximal convoluted renal tubule (Kovacs *et al.*, 1997). This is a malignant neoplasm composed of cells with clear or eosinophilic cytoplasm within a fragile vascular network (Figure 3, **A**) (Eble *et al.*, 2004).

Loss of sequences at chromosome 3p is a characteristic somatic genetic feature in the vast majority of sporadic clear cell RCC (Teyssier *et al.*, 1986). This finding suggests the presence of one or more TSG relevant for RCC development on this chromosomal arm. The *VHL* tumor suppressor gene is one of the genes located at 3p and biallelic *VHL*

inactivation is seen in a high proportion of RCCs. This inactivation follows the Knudson's two-hit model, and may occur through mutation (34-56% of the cases), deletion or promoter methylation (19% of the cases) (Bodmer *et al.*, 2002).

The VHL protein acts by down-regulating the hypoxia-inducible factor, which is responsible for the activation of genes involved in several cellular processes, such as proliferation, neo-vascularization, and extracellular matrix formation (Eble *et al.*, 2004).

3.2 Papillary Renal Cell Carcinoma

Papillary RCC (pRCC) is encountered in 10 to 15% of nephrectomy series (Fleming, 2000), thus being the second most common carcinoma of the kidney. It is a malignant parenchymal neoplasm with papillary or tubulopapillary architecture (Figure 3, **B** and **C**) (Eble *et al.*, 2004) and has a less aggressive clinical course compared to clear cell RCC (Lopez-Beltran *et al.*, 2009).

pRCC is classified in two different subtypes, type I (Figure 3, **B**) and type II (Figure 3, **C**), depending on the morphology of the tumor cells covering the papillary lesions. This renal cell tumor, like ccRCC, arises from cells in the proximal convoluted renal tubule (Kovacs *et al.*, 1997). The commonest karyotypic alterations associated with this carcinoma are trisomies of chromosomes 7 and 17, and Y chromosome loss. Trisomy of chromosomes 12, 16 and 20 are also found and may be related to tumor progression (Eble *et al.*, 2004). pRCC also exhibits somatic mutations of the *MET* proto-oncogene, which encodes a tyrosine kinase growth factor receptor for hepatocyte growth factor located on chromosome 7 (Schmidt *et al.*, 1997).

3.3 Chromophobe Renal Cell Carcinoma

The third most common RCC subtype is chromophobe RCC (chrRCC), which is a less aggressive type of RCC (Lopez-Beltran *et al.*, 2009), accounting for 5% of all renal neoplasms. It is thought to arise from the renal collecting duct cells (Bodmer *et al.*, 2002), and is usually characterized by large pale cells with prominent cell membranes (Figure 3, **D** and **E**) (Eble *et al.*, 2004).

This tumor type is genetically characterized by massive chromosomal loss, most frequently of chromosomes 1, 2, 6, 10, 13, 17 and 21 (Eble *et al.*, 2004).

3.4 Oncocytoma

Oncocytoma is a benign renal epithelial tumor with large cells containing mitochondria-rich eosinophilic cytoplasm, thought to arise from intercalated duct cells (Figure 3, **F**). It comprises of about 5% of all renal tumors arising from tubular epithelium (Eble *et al.*, 2004).

In terms of somatic genetics, they usually display a mixed population of cells with normal and abnormal karyotypes. Some cases show the translocation t(5;11)(q35,q13) while others show loss of chromosomes 1 and 14 (Eble *et al.*, 2004). Alterations in mitochondrial DNA is also a frequent feature of these tumors (Lopez-Beltran *et al.*, 2009).

3.5 Distinction among renal tumor subtypes

Chromophobe RCC was first described in 1985 by Thoenes *et al.* and consists of two main variants, classical and eosinophilic, that can ultimately present overlapping features with both clearly malignant and benign renal tumors. The classical variant (Figure 3, **D**) is characterized by large polygonal cells with transparent, slightly reticulated cytoplasm and can be hard to distinguish from clear cell RCC. The eosinophilic variant (Figure 3, **E**), composed of intensely eosinophilic cells resembles oncocytoma (Thoenes *et al.*, 1988).

Since chromophobe RCC is a distinct type of renal cell carcinoma with an overall prognosis and biological behavior significantly better than those of clear cell RCC, although worse than those of oncocytoma, it is clinically important to make an appropriate distinction between these specific subtypes of renal neoplasms.

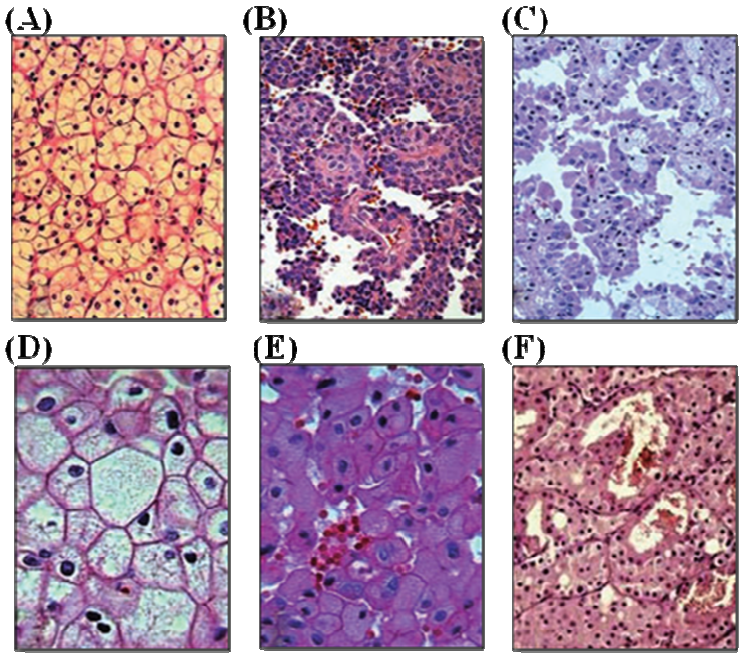

Figure 3: Main histologic types of renal cell tumors. **(A)** Clear cell Renal Cell Carcinoma; **(B)** Papillary Renal Cell Carcinoma, type I; **(C)** Papillary Renal Cell Carcinoma, type II; **(D)** Chromophobe Renal Cell Carcinoma, classical variant; **(E)** Chromophobe Renal Cell Carcinoma, eosinophilic variant; **(F)** Oncocytoma. *Adapted from (Lopez-Beltran et al., 2009).*

3.6 Clinical and Pathological staging

One of the most frequently used staging systems is the American Joint Committee on Cancer (AJCC) tumor-node-metastases (TNM) staging system. This classification system provides a defined description of the tumor, area and extent of invasion, and degree of vascular involvement. These criteria for tumor staging results in the grouping of RCC cases into four different stages (Nguyen and Campbell, 2006).

Table 1 shows detailed information on TNM staging for kidney cancer.

Table 1: TNM staging and stage gouping for kidney cancer.

T – Primary tumor	
TX	Primary tumor cannot be assessed
T0	No evidence of primary tumor
T1	Tumor 7 cm or less in greatest dimension, limited to the kidney
T1a	Tumor 4 cm or less in greatest dimension, limited to the kidney
T1b	Tumor more than 4 cm but not more than 7cm in greatest dimension, limited to the kidney
T2	Tumor more than 7 cm in greatest dimension, limited to the kidney
T2a	Tumor more than 7 cm but less than or equal to 10 cm in greatest dimension, limited to the kidney
T2b	Tumor more than 10 cm, limited to the kidney
T3	Tumor extends into major veins or perinephric tissues but not into the ipsilateral adrenal gland and not beyond Gerota's fascia
T3a	Tumor grossly extends into the renal vein or its segmental (muscle containing) branches, or tumor invades perirenal and/or renal sinus fat but not beyond Gerota's fascia
T3b	Tumor grossly extends into vena cava below the diaphragm
T3c	Tumor grossly extends into vena cava above the diaphragm or invades the wall of the vena cava
T4	Tumor invades beyond Gerota's fascia (including contiguous extension into the ipsilateral adrenal gland)
N – Regional Lymph Nodes	
NX	Regional lymph nodes cannot be assessed
N0	No regional lymph node metastasis
N1	Regional lymph node metastasis
M – Distant metastasis	
M0	No distant metastasis
M1	Distant metastasis
Stage grouping	
Stage I	T1 N0 M0
Stage II	T2 N0 M0
Stage III	T1 or T2 N1 M0 / T3 N0 or N1 M0
Stage IV	T4 Any N M0 / Any T Any N M1

Adapted from AJCC Cancer Staging Manual, 2010 (Edge et al., 2010).

3.7 Histopathological grading

Grading of RCC is based on the Fuhrman system, consisting of four grades. This grading system is based on the nuclear size, contour and conspicuousness of nucleoli (Fuhrman *et al.*, 1982) and is the most important prognostic predictor in RCC, mainly for the clear cell type (Lopez-Beltran *et al.*, 2009).

3.8 Tumor prognosis

There has been a gradual improvement in RCC prognosis over the last decades, with 5-year relative survival rates as high as 64% in 2002, compared with less than 40% in the early 1960s (Baldewijns *et al.*, 2008).

Factors influencing prognosis can be classified into anatomical, histological, clinical, and molecular. Anatomical factors are usually included in the TNM staging classification system. The histological factors include the Fuhrman grade, RCC subtype, presence of sarcomatoid features, microvascular invasion, tumor necrosis and invasion of the collecting system. Clinical factors consist of patient performance status, localized symptoms, anaemia and platelet count. Finally, and concerning the molecular factors, numerous molecular markers have been investigated. However, to date, none of these markers has provided evidence to improve the predictive accuracy of existing prognostic systems (Ljungberg *et al.*, 2010).

In univariate analysis, there is a trend towards a better prognosis for patients with chrRCC when compared with pRCC and ccRCC. However, in multivariate analysis, TNM stage, Fuhrman grade and the performance status, but not histology, are preserved as independent prognostic variables. Tumor necrosis is also a strong independent predictor of poor outcome for ccRCC but not for chrRCC or pRCC. Microvascular invasion and presence of sarcomatoid features are also reported as adverse prognostic indicators (Baldewijns *et al.*, 2008).

The clinical behavior of RCC depends on complex interactions between several prognostic factors, however the currently available most useful predictors of patient outcome include patient performance status, tumor stage and grade (Baldewijns *et al.*, 2008).

4. Epigenetics

The term "epigenetics" remounts to the fourth decade of the 20th century and was first referred as gene-environment interactions that ultimately lead to a particular phenotype. Waddington originally used this word in a developmental context to define the changes in gene activation and deactivation necessary for cellular differentiation (Franklin and Mansuy, 2009). Nowadays, the term refers to both mitotically and/or meiotically heritable changes in gene expression that are not accompanied by changes in the DNA sequence (Jones and Baylin, 2007).

The epigenetic processes that stably alter gene expression patterns result from modifications of the DNA molecule or chromatin structure and include DNA methylation, post-translational histone modifications, and changes in microRNA patterns (Mulero-Navarro, 2008).

4.1 DNA Methylation

DNA methylation is the most well studied epigenetic change. This modification occurs in almost all living organisms, from bacteria to plants and animals (Scarano *et al.*, 2005) and is suggested to lead to transcriptional silencing via several mechanisms (Gibney and Nolan, 2010).

In the mammalian genome, methylation occurs essentially at cytosine bases that precede a guanosine, in the so-called CpG dinucleotides, where the 'p' represents the phosphodiester bond linking cytosine- and guanosine-containing nucleotides. These CpG dinucleotides are not randomly distributed in the genome, being preferentially located in short regions of 0.5 – 4 kb in length, known as CpG islands (Jones and Baylin, 2002). The majority of CpG islands can be found near the promoter regions of several genes and approximately 60% of human genes contain these CpG islands (Antequera and Bird, 1993).

DNA methylation is conducted by a family of DNA methyltransferase enzymes (DNMTs) that work through covalent addition of a methyl group to the fifth carbon position of cytosines (Lopez-Serra and Esteller, 2008) (Figure 4). Various DNMTs, with different specificities have been already described: DNMT1, the main enzyme that maintains DNA methylation during replication, showing preference for hemi-methylated DNA substrates; DNMT3a and DNMT3b which are involved in the generation of new

methylation patterns, targeting unmethylated CpG dinucleotides, and finally DNMT2 whose biological function is not very well established (Mulero-Navarro, 2008).

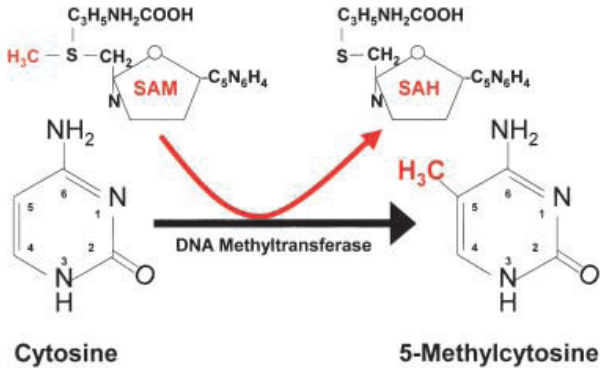

Figure 4: Formation of a 5-methylcytosine. A DNA methyltransferase enzyme catalyzes the transfer of a methyl group (CH_3) from S-adenosylmethionine (SAM) to (deoxy)cytosine, producing 5-(deoxy)methylcytosine and S-adenosylhomocystine (SAH). *Adapted from (Attwood et al., 2002).*

In vertebrates, more than 80% of CpG dinucleotides that are not located in the CpG islands are frequently methylated. However, those within CpG islands are usually not methylated or show relatively low levels of methylation (Gibney and Nolan, 2010).

In normal cells, DNA methylation is involved in processes such as gene dosage reduction in X-chromosome inactivation in females and genomic imprinting. Methylation also occurs at repetitive DNA sequences to promote chromosome stability (Lopez-Serra and Esteller, 2008).

DNA methylation is accompanied by histone modifications that regulate chromatin structure and together they determine the transcriptional state of the DNA. Histones can be modified by acetylation, methylation, phosphorylation, glycosylation, sumoylation and ADP ribosylation, but the most frequent modifications are acetylation and methylation of lysine residues in the amino terminal of histone 3 and histone 4 (Bollati and Baccarelli, 2010). Such modifications act sequentially or in combination to specify the “histone code”. The communication between DNA methylation and histone modifications probably occurs in both directions and might be partially mediated by nuclear factors with methyl DNA binding activity, such as the MBD (Methyl-CpG-binding domain) proteins. These proteins recognize single methylated CpG dinucleotides and are capable of recruiting histone modifying and chromatin remodeling complexes to the methylated sites (Figure 5) (Lopez-Serra and Esteller, 2008).

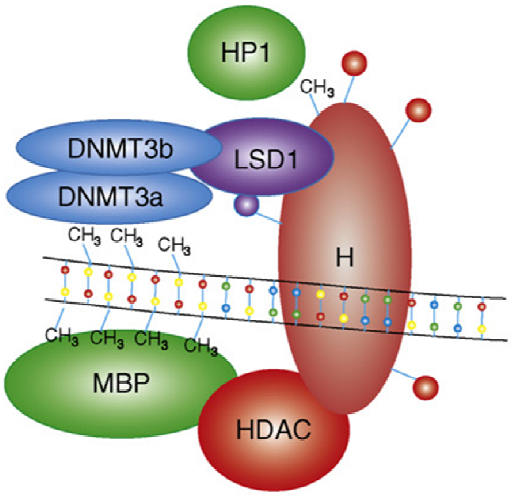

Figure 5: Interplay between DNA methylation and histone modifications. MBPs bind to regions of methylated DNA and form complexes with histone deacetylases, HDACs. Similarly, proteins that either bind to modified histones (*e.g.*, heterochromatin protein 1, HP1) or directly modify histones (*e.g.*, lysine-specific demethylase 1, LSD1), recruit DNMTs to induce DNA methylation. **DNMT**: DNA methyltransferase, **MBP**: Methyl-CpG- binding protein, **HDAC**: Histone deacetylase, **H**: Histone, **LSD1**: Lysine-specific demethylase, **HP1**: heterochromatin protein 1. *Adapted from (Handel et al., 2010).*

4.2 Methylation patterns in cancer

In cancer cells, DNA methylation patterns are deeply altered (Figure 6). The cause of such alteration is not fully understood but could result from local alterations in DNMTs, which are expressed at higher levels in tumor cells (Jones and Baylin, 2002).

The first epigenetic modification to be identified in cancer cells was an overall decrease of CpG methylation. The mechanisms that may explain the involvement of this global DNA hypomethylation with the onset and progression of cancer is the generation of chromosome instability, the reactivation of transposable elements and the loss of imprinting (Esteller, 2008). *IGF2* (Insulin-like growth factor 2) and *H19* are two well known examples of imprinted genes that become hypomethylated and are consequently overexpressed in cancer (Ehrlich, 2009).

On the other hand, another frequent and early event in cancer is aberrant promoter methylation of tumor suppressor genes, which leads to their silencing and eventually to the development of the carcinogenic process. These genes are usually involved in cell cycle regulation, DNA repair, apoptosis, angiogenesis, invasion and adhesion (Lopez-Serra and Esteller, 2008).

Loss of *GSTP1* expression, the gene encoding the drug detoxification enzyme gluthatione S-transferase π (GST- π), is frequently observed in prostate cancer and this gene silencing is directly associated with aberrant promoter methylation (Jeronimo *et al.*, 2001). This is an example of a gene that acts as a caretaker, protecting prostate cells against genomic damage mediated by a variety of oxidants. Thus, its loss predisposes normal prostatic cells to DNA damage leading to carcinogenesis (Costa *et al.*, 2007a).

Some CpG islands, associated with proto-oncogenes promoter regions, are methylated in non-neoplastic somatic cells. Therefore, in cancer cells, these promoter regions may become demethylated causing repressed oncogenes to be re-activated and/or overexpressed. *HRAS* (Harvey rat sarcoma viral oncogene homolog) and *cMYC* (Myelocytomatosis viral oncogene homolog) are some of the examples of this kind of gene re-activation associated to CpG islands loss of methylation. These activated oncogenes might be implicated in the onset of cellular transformation and/or tumor progression (Scarano *et al.*, 2005) but evidence suggests a larger involvement in the activation of genes associated with tumor invasion and metastasis (Ehrlich, 2009).

Aberrant promoter methylation patterns have also been reported to be involved in miRNA silencing. miRNAs are small non-coding RNAs that target specific genes and silence its protein expression. In cancer, the expression patterns of these miRNAs are profoundly altered (Lopez-Serra and Esteller, 2008).

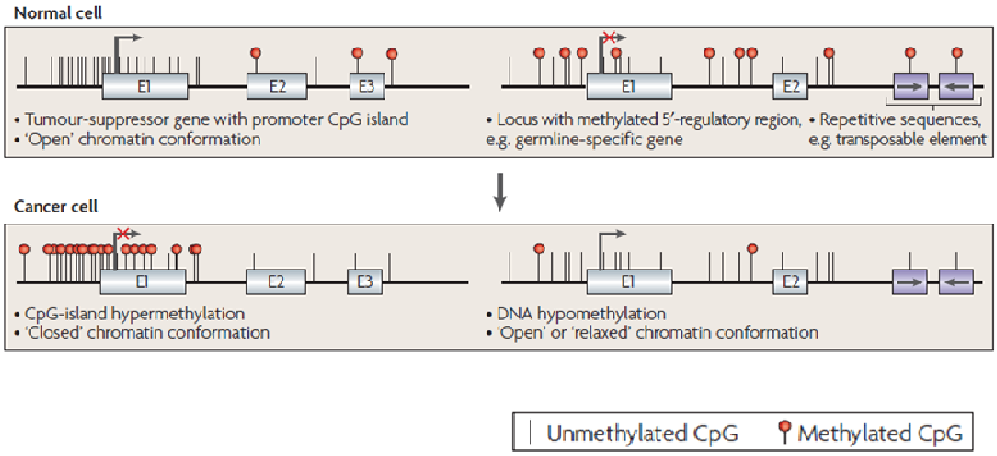

Figure 6: DNA methylation patterns in normal and in cancer cells. **E**, exon.
Adapted from (Esteller, 2007).

4.3 Epigenetics in renal cell tumors

Mutations and deletions do not cover 100% of the alterations found in sporadic and heritable RCC cases, and therefore aberrant gene promoter methylation (hyper- and hypo-) is thought to be an alternative event underlying at least some of the cases. In this respect, information concerning the gene methylation profile of renal cell carcinomas is relatively limited.

Some candidate tumor suppressor genes (TSGs) silenced by hypermethylation have already been reported to be associated with RCC. A very good example of such a gene is the *VHL* tumor suppressor gene. Herman and colleagues first reported *VHL* promoter hypermethylation associated with gene silencing (Herman *et al.*, 1994), as an alternative inactivation mechanism in a proportion of sporadic ccRCC cases.

Another frequent event, described by Morris *et al.*, is the methylation of the gene coding the transmembrane chemokine *CXCL16* in RCC cell lines and in primary tumors but not in normal kidney (Morris *et al.*, 2008). In addition to these genes many other TSGs have been investigated. Several adhesion molecules (e.g. *CDH1*, *JUP*, *LSAMP*), genes associated with apoptosis (e.g. *APAF1*, *CASP8*, *DAPK1*), cell cycle genes (e.g. *CDKN2α*), among others, have been described to be methylated in RCC, although revealing variable methylation frequencies (Baldewijns *et al.*, 2008).

Another reported event is the activation of the *MN/CA9* gene that has been associated with hypomethylation in human renal cell carcinoma cell lines (Cho *et al.*, 2000).

Epigenetic alterations, particularly promoter methylation, are also an important class of cancer biomarkers. Costa *et al.* described in 2007 three differentially methylated cancer-related genes, *CDH1*, *PTGS2* and *RASSF1A*, in the four most prevalent renal cell tumor subtypes, ccRCC, pRCC, chrRCC and oncocytoma (Costa *et al.*, 2007b).

5. The *PAX* Gene Family

The paired-box transcription factor family, encoded by developmental control genes, is mainly characterized by a highly conserved paired-box DNA-binding domain. This domain was initially identified in the *Drosophila* pair-rule segmentation gene *paired* (*prd*).

Nine paired-box genes have been described until now (*PAX1* to *PAX9*), which can be divided into four different subgroups. This classification is based on the gene sequence and

correlates with expression patterns in developing embryonic tissues (Chi and Epstein, 2002).

The temporal and spatial expression of *PAX* genes is tightly regulated as PAX proteins function as nuclear transcription factors essential not only for cellular differentiation, and migration, but also for cell proliferation. Since these genes are important transcriptional regulators it is likely that they are relevant targets for disruption during oncogenesis (Schafer, 1998).

5.1 *PAX2* Gene

The *PAX2* (*Paired-box 2*) gene encodes a transcription factor belonging to the evolutionarily conserved paired-box family. It is required during the development of the central nervous system and genitourinary tract (Torban *et al.*, 2000), being expressed in the developing kidney as well as the optic stalk, midbrain-hindbrain junction, and the spinal chord (Chi and Epstein, 2002).

5.1.1 Molecular characterization

The *PAX2* gene, along with *PAX5* and *PAX8*, belongs to subgroup II of the *PAX* family and is located at locus 10q24.3-q25.1 (Figure 7).

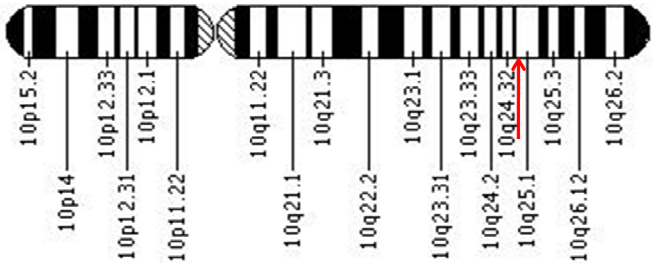

Figure 7: Chromosome 10 mapping. Red arrow indicates *PAX2* gene location in chromosome 10. *Adapted from Genetics Home Reference (Calvo et al., 2010).*

The *PAX2* gene contains 12 exons (Sanyanusin *et al.*, 1996), several of which are alternatively spliced. There are 5 well characterized alternative splice variants (variant 1 to 5) which encode 5 different isoforms (isoforms *a* to *e*) (Figure 8).

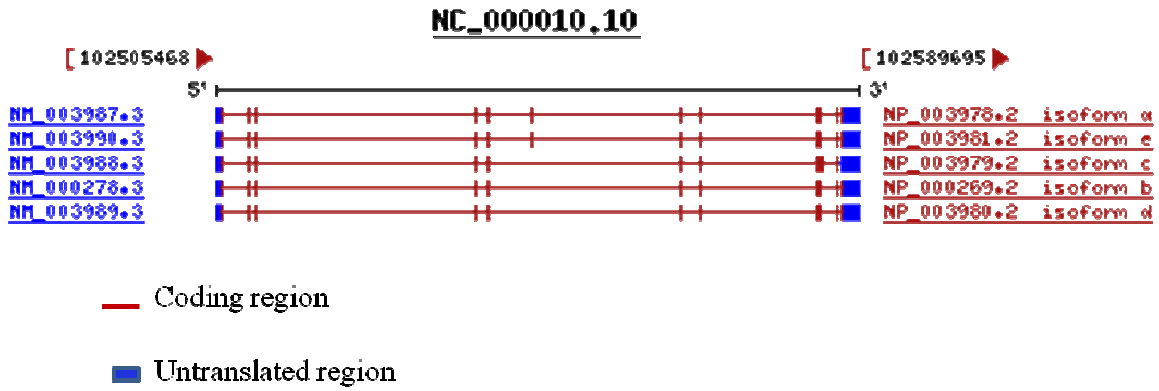

Figure 8: *PAX2* transcript variants.
Adapted from (NCBI, 2010).

Transcript variant *e* encodes the longest isoform. The variant *b* lacks an alternate in-frame exon and uses an alternate splice site in the 3' coding region, compared to variant *e* resulting in a protein (isoform *b*) with a shorter, distinct C-terminus compared to isoform *e*. Variant *a* uses an alternate in-frame splice site in the 3' coding region, compared to variant *e*, resulting in a shorter protein (isoform *a*) that has a shorter, distinct C-terminus compared to isoform *e*. Variant *c* has multiple differences in the coding region, compared to variant *e*, one of which results in a translational frameshift. The resulting protein (isoform *c*) has a distinct C-terminus, with a proline-, serine-, threonine-rich portion, and is shorter than isoform *e* because it also lacks exon 6. Transcript variant *d* lacks an alternate in-frame exon compared to variant *e*. This results in an isoform (isoform *d*) that is shorter than isoform *e* (Ward *et al.*, 1994). Importantly, all transcript variants share the same promoter region.

5.1.2 The PAX2 *protein*

The PAX2 protein is composed by 434 amino acid residues and has a nuclear localization. PAX proteins can mediate DNA binding and either transcriptional activation or repression through distinct domains. The PAX2 protein, specifically, has three distinct domains: an amino-terminal paired-box domain (PD), a conserved octapeptide domain (OP) and a proline-serine-threonine-rich carboxy-terminal transactivation domain (TD) (Figure 9, **A**). There is a fourth domain, the paired-type homeodomain (HD), which is truncated to a single helix among the proteins belonging to the subgroup II of PAX proteins, in which PAX2 is included (Figure 9, **A** and **B**) (Dressler *et al.*, 1990; Eccles *et al.*, 1992; Wang *et al.*, 2008).

(A)

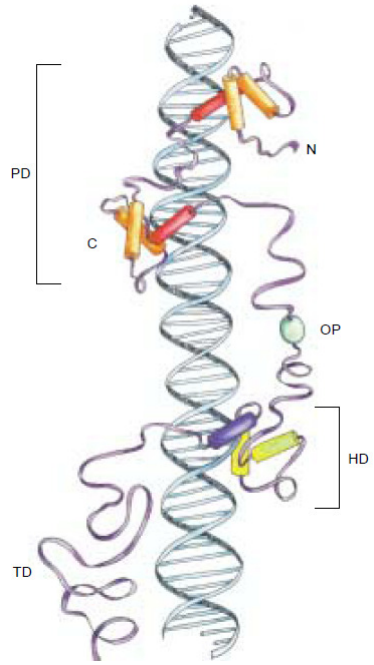

(B)

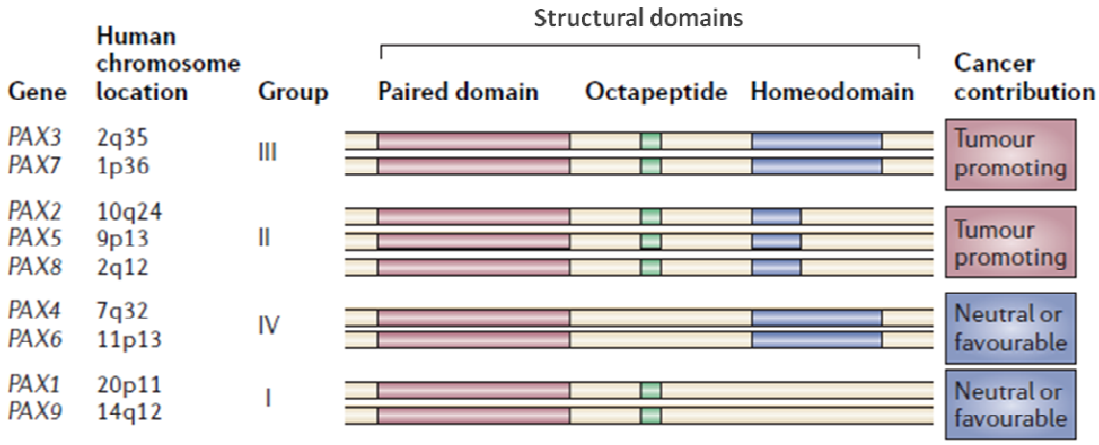

Figure 9: **(A)** Structural representation of a PAX family protein containing the paired-domain (PD), the octapeptide motif (OP), the homeodomain (HD) and the transactivation domain (TD). *In Chi and Epstein, 2002*. **(B)** Schematic representation of the structural domains of the *PAX* gene family groups, and their putative contribution to cancer. *In (Robson et al., 2006).*

DNA binding activities are associated with the amino terminal paired-box domain, and transcription activation or repression are mediated by C-terminal domains of the PAX2 protein (Lechner and Dressler, 1996). More specifically, the PD, composed of 128 amino acid residues, establishes high affinity sequence-specific interactions with DNA (Wang *et*

al., 2008). Structurally, this domain is composed of three α-helices, two of which are located near the carboxy end and the other near to the amino end of the domain (Stuart and Gruss, 1996). The OP motif is located between the PD and the HD (reduced to a single helix in PAX2). It has been described that this motif mediates transcriptional inhibition, thus acting like a repressor (Eberhard *et al.*, 2000). The TD has also been shown to exert transcriptional regulation function (Chi and Epstein, 2002).

The presence of both activation and repression domains in PAX2, as well as in the other PAX family members, suggests that these proteins have multiple functions that ultimately depend on the cellular context of target sequences (Dressler and Woolf, 1999).

The proteins included in subgroups II (PAX2, PAX5 and PAX8) and III (PAX3 and PAX7) play key roles in human malignancies (Figure 9, **B**). The proteins included in both of these subgroups comprise an octapeptide domain (OP), and at least a partial homeodomain (HD), as can be seen in Figure 9, **B**. Therefore it would be plausible to postulate that both these domains may be involved in the interaction with a specific network of proteins and that this interaction might turn those genes more susceptible to inappropriate regulation within a tumor cell microenvironment (Robson *et al.*, 2006).

6. PAX2 in Kidney Development

Three partially overlapping kidney systems are formed during human embryonic development: the pronephros, the mesonephros and metanephros. The first two systems are transient and the third persists as a functional kidney appearing in the 5th week of embryonic development in humans (Sadler, 2004). Like most organs, differentiation of the kidney involves epithelial-mesenchymal interactions. In this organ, the epithelium of the ureteric bud (UB) from the mesonephros interacts with mesenchyme of the metanephric blastema (Metsuyanim *et al.*, 2008).

In the first steps of the metanephros development, the metanephrogenic mesenchyme develops and induces the formation of epithelial branches, the ureteric buds. When the these emerge they enter the metanephric mesenchyme inducing this mesenchymal tissue to condense around them and differentiate into the nephrons (Figure 10). First, the tips of these branches induce the mesenchyme cells to form epithelial aggregates or vesicles, which will give rise to small S-shaped tubules (Gilbert, 2003). Then, capillaries grow into

the pocket at one end of the S and differentiate into glomeruli. The tubes derived from the mesenchyme form the secretory nephrons of the functional kidney and the branched ureteric bud gives rise to the renal collecting ducts and to the ureter. The tubules and the glomeruli constitute the nephrons. The proximal end of each of the nephrons forms the Bowman's capsule that grows around the glomerulus. These two structures constitute the renal corpuscle. Continuous lengthening of the excretory tubule results in formation of the proximal convoluted tubule, loop of Henle and distal convoluted tubule (Sadler, 2004).

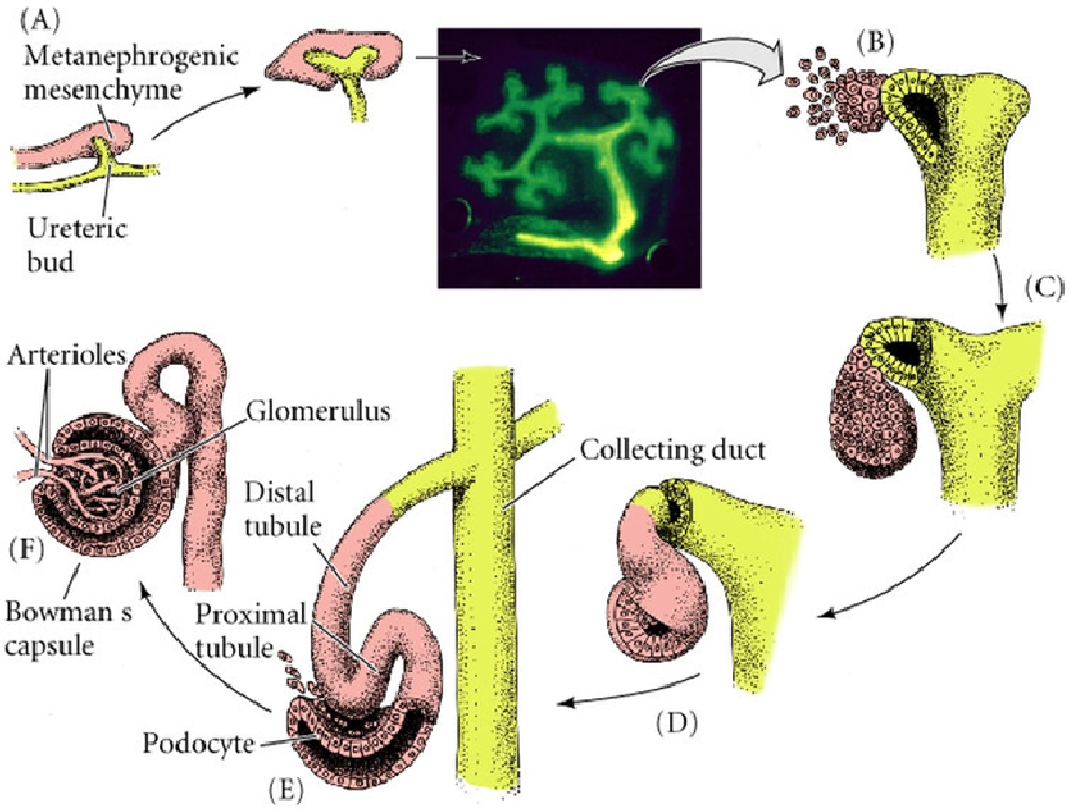

Figure 10: Representative scheme of the developing kidney.

(A) The two intermediate mesodermal tissues - the UB and the metanephrogenic mesenchyme – interact and induce each other to form the kidney; the metanephrogenic mesenchyme induces the UB to elongate and branch. **(B)** The tips of these branches cause the mesenchyme cells to aggregate. **(C)**, **(D)** Each aggregated nodule first elongates and then forms a characteristic S-shaped tubule. **(E)**, **(F)** The cells of this epithelial structure begin to differentiate into specific cell types to form the mature structure.

Adapted from (Gilbert, 2003).

Several genes have been identified that are expressed in the undifferentiated metanephric mesenchyme, and are required for appropriate differentiation of the metanephric kidney. These include *PAX2*, *WT1* (Wilms tumor 1), *EYA* (Eyes absent

homolog 1), *SIX2* (SIX homeobox 2), *HOX11* (*TLX1*, T-cell leukemia homeobox 1), among others (Metsuyanim *et al.*, 2008).

Paired-box domain containing gene products are transcriptional factors and are thus capable of implementing a genetic program. These PAX proteins have been shown to play an essential role in early mammalian development (Stuart and Gruss, 1996). In the case of *PAX2*, specifically, both mRNA and protein can be detected in the pronephric duct, the earliest epithelial structure derived from the intermediate mesoderm. As the duct extends into the mesonephric region, *PAX2* expression remains and becomes evident in mesonephric tubules. At the time of ureteric bud outgrowth and invasion into the metanephric mesenchyme, *PAX2* expression is activated in mesenchymal cells with particular high levels in condensing mesenchyme at the UB tips, where it is thought to suppress apoptosis and promote epithelial aggregation. This process is critical to achieve the optimal nephron number at birth (Dziarmaga *et al.*, 2006a). *PAX2*, together with *WNT4* (Wingless-type MMTV integration site family, member 4), causes the mesenchyme to epithelialize in preparation for tubule differentiation (Sadler, 2004). Thus, the *PAX2* is one of the earliest markers for induced mesenchyme and may be activated by inductive signals that come from the bud (Dressler and Woolf, 1999). It seems that PAX2 also orchestrates the branching of the UB through activation of glial derived neurotrophic factor (*GDNF*) and its corresponding receptor (Brophy *et al.*, 2001).

The *PAX2* expression, primarily seen during the early stages of development, seems to be switched off in the later phases of terminal differentiation, in the most part of the kidney structures. In fact, as the induced mesenchyme suffers epithelial conversion forming first the renal vesicle and then the S-shaped body, *PAX2* expression is down-regulated (Dressler and Woolf, 1999). In adult kidneys, PAX2 protein expression is restricted to collecting ducts, being almost undetectable in the proximal and distal tubules. *PAX2* expression in collecting ducts protects medullary cells against the stress induced by high levels of NaCl and urea. The stress of hyperosmolality is a great stimulus for *PAX2* induction in the renal medulla *in vivo* (Cai *et al.*, 2005).

How *PAX2* expression is suppressed at the end of embryogenesis in most of these structures remains unclear, but some data support that epigenetic silencing, mediated by *PAX2* promoter methylation, occurs in the normal adult kidney cells of rats (Metsuyanim *et al.*, 2008).

Germline mutations in *PAX2* gene lead to developmental abnormalities in kidneys, as well as in other organs (Fletcher *et al.*, 2005) revealing the important role of *PAX2* in kidney development.

7. PAX2 Protein Interactions

There is evidence that PAX proteins' function must be mediated by interactions with other nuclear proteins. These nuclear proteins should be able to complex with PAX2 at the DNA binding site and thus mediate activation or repression (Dressler and Woolf, 1999).

McConnell and colleagues described that PAX2 binds to WT1 5' regulatory sequences, and that these two proteins work by cross transcriptional control: at the early stages of renal development PAX2 modulates the transcriptional activity of WT1; at later stages, when a threshold level of WT1 is reached, it represses PAX2 transcription (McConnell *et al.*, 1997). The Wilms tumor suppressor gene, *WT1*, is a transcription factor expressed in the fetal kidney condensed mesenchyme that makes this tissue competent to respond to induction by the UB. The bud induces the mesenchyme via *FGF-2* (Fibroblast growth factor 2) and *BMP-7* (Bone morphogenetic protein 7) (Sadler, 2004).

Other researchers reported that activin, a dimeric protein, member of the TGFβ superfamily, is involved in the disruption of the ureteric bud branching, thus being a negative regulator of tubulogenesis, and reduces PAX2 expression in embryonic kidneys (Maeshima *et al.*, 2002).

Neuronal apoptosis inhibitor protein (NAIP) is an endogenous inhibitor of caspases 3 and 7, expressed in the UB of the fetal kidney. Its expression pattern overlaps that of PAX2. Some studies showed that PAX2 binds directly to a motif in the NAIP promoter stimulating its transcription *in vitro* (Dziarmaga *et al.*, 2006b).

The BRCT-domain protein PTIP (PAX transcription activation domain interacting protein) links PAX2 to the H3K4 methylation machinery. PTIP is part of a histone H3K4 methyltransferase complex that localizes to a PAX2 DNA binding sequence, in a PAX2 dependent way, recruiting the ALR methyltransferase complex to the PAX2 binding site (Patel *et al.*, 2007). Because PAX2 can be serine/threonine phosphorylated in response to Wnt signals, the interaction with PTIP promotes H3K4 methylation at kidney-specific loci in response to inductive signals (Dressler, 2008).

A recent study also suggested that the activation of *PAX2* is stimulated by hypoxia and depends on the functional integrity of *VHL* in ccRCCs (Luu *et al.*, 2009). These authors identified several putative hypoxia response elements by analyzing the *PAX2* promoter region, and showed that *PAX2* activation is essentially regulated by HIF, although other tissue specific factors may be required for its expression in these tumors (Luu *et al.*, 2009).

8. *PAX2* as a Proto-oncogene

The oncogenic potential of the *PAX* genes family has been reported *in vitro* with transformation of cell cultures and *in vivo* with cell injections in nude mice (Maulbecker and Gruss, 1993).

Several members of the *PAX* family, especially those corresponding to subgroup II and III, are involved in a number of human malignancies including renal tumors, lymphoma, thyroid medullary carcinoma, rhabdomyosarcoma and melanoma (Muratovska *et al.*, 2003). PAX2 expression in particular, has been detected in primary tumor sections of brain, breast, ovarian, and lymphoid cancer (Muratovska *et al.*, 2003). Other authors have also reported *PAX2* expression in renal cell, endometrial and prostate carcinoma (Gnarra and Dressler, 1995; Wu *et al.*, 2005; Bose *et al.*, 2009).

As previously stated, the expression of PAX2 protein is not observed in the mature renal structures, except for the collecting ducts. In Wilms tumors, a relatively common childhood neoplasm, and in some of the subtypes of renal cell tumors, re-expression of PAX2 can be detected by immunohistochemistry (Metsuyanim *et al.*, 2008; Gupta *et al.*, 2009). In these RCT subtypes expressing PAX2, namely clear cell RCC, papillary RCC and oncocytoma, PAX2 expression may be part of the tumorigenic process representing a proliferation stimulus (Figure 11). On the other hand, failure to suppress *PAX2* during embryonic development may predispose renal epithelial cells to further genetic lesions in a multistep oncogenic transformation pathway (Gnarra and Dressler, 1995).

In fact, there is evidence supporting that PAX2 protects against caspase-2-induced apoptosis in renal collecting duct cells (Figure 11), which are those expressing PAX2 in normal adult kidneys (Torban *et al.*, 2000), and suggest the involvement of PAX2 in cell

proliferation and differentiation to reconstruct tubular structure during regeneration after ischemic injury (Maeshima *et al.*, 2002).

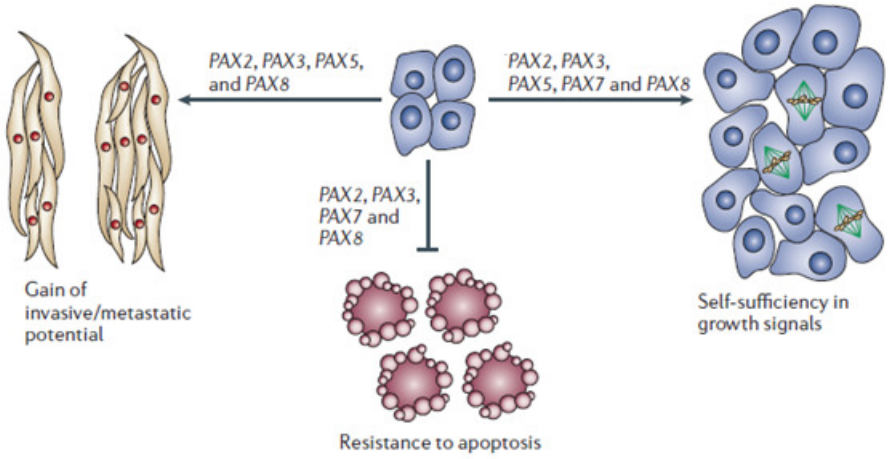

Figure 11: Characteristics conferred by *PAX2* gene, and other *PAX* family members, that promote tumor formation and/or progression. *Adapted from (Robson et al., 2006).*

In 2006, Hueber and colleagues reported that PAX2 conferred resistance to cisplatin-induced apoptosis. Cisplatin is a widely used anticancer drug that interacts with DNA forming adducts and therefore induces several signal transduction pathways that ultimately result in the activation of apoptosis (Hueber *et al.*, 2006). Others have also reported that the expression of PAX2 by Kaposi's sarcoma cells correlates with an enhanced resistance to vincristine-induced apoptosis and promotes invasive potential (Buttiglieri *et al.*, 2004).

All these data are in agreement with the already stated idea that *PAX2* may act as an oncogene, by stimulating cell proliferation and/or by inhibiting apoptosis. These characteristics conferred by *PAX2* gene are depicted in Figure 11.

9. Methylation of *PAX* Genes

Several members of the *PAX* genes family have been described to be aberrantly methylated in different cancer models. These genes are involved in numerous steps of carcinogenesis and may work either as TSGs or as proto-oncogenes.

The promoter of *PAX6*, a gene coding for a DNA binding protein that participates in brain and eye development, has been described to be aberrantly methylated in early bladder cancer and in normal adjacent mucosa (Hellwinkel *et al.*, 2008). Other investigators found

that this gene promoter was methylated in a tumor cell line and in primary tumors from follicular lymphoma (Bennett *et al.*, 2009).

The *PAX5* gene belongs to the same PAX family group as *PAX2* and participates in cell differentiation and embryonic development. This gene has also been reported to be a frequent target for aberrant methylation in tumor cell lines, as well as in primary tumors from breast and lung (Palmisano *et al.*, 2003).

PAX7 belongs to group III of *PAX* genes family, which is considered a tumor promoting group of genes. This gene has also been reported to be methylated in RL follicular lymphoma cell line (Bennett *et al.*, 2009).

Concerning *PAX2*, Wu and colleagues have described *PAX2* promoter hypomethylation in endometrial carcinoma as being responsible for PAX2 re-expression in this type of cancer. These authors showed that the *PAX2* promoter was methylated in normal endometrium and that this methylation was concomitant with lack of *PAX2* expression. On the other hand, endometrial carcinomas showed *PAX2* promoter hypomethylation, and this state was correlated with *PAX2* expression (Wu *et al.*, 2005). Moreover, Metsuyanim *et al.* reported *PAX2* hypermethylation in the adult kidney of rats coinciding with its silencing with the completion of nephrogenesis (Metsuyanim *et al.*, 2008).

AIMS OF THE STUDY

According to the literature, significant expression of PAX2 protein occurs in three of the most prevalent renal cell tumor subtypes - clear cell RCC, papillary RCC and oncocytoma - but not in chromophobe RCC (Gupta *et al.*, 2009). Moreover, *PAX2* is considered an oncogene, suppressed at the later stages of embryonic development, possibly by promoter methylation (Metsuyanim *et al.*, 2008), and reactivated during the carcinogenic process of some cancer models. Therefore, we hypothesized that PAX2 loss of expression in chromophobe RCC might be due to epigenetic silencing, through promoter methylation.

On the other hand, both fluorescent in situ hybridization (FISH) (Brunelli *et al.*, 2005) and conventional cytogenetic (Memeo *et al.*, 2007) analysis showed that chromosome 10 loss occurs in 40 to 60% of chromophobe RCC cases. Because *PAX2 locus* maps to chromosome 10, gene deletion might constitute an alternative mechanism for gene downregulation.

Hence, the main goal of this study was to identify epigenetic and/or genetic alterations affecting the *PAX2* gene in a series of renal cell tumors, representing the four major subtypes: clear cell RCC, papillary RCC, chromophobe RCC, and oncocytoma.

Specifically, the aims of this study were to:

1. Analyze the expression of *PAX2* in the different renal cell tumor subtypes, at mRNA level and at protein level.
2. Determine whether the regulation of *PAX2* expression occurs by epigenetic mechanisms, by assessing its promoter methylation status.
3. Analyze the association between the number of *PAX2* copies and its expression in a series of renal cell tumors.
4. Evaluate the potential use of *PAX2* epigenetic/genetic alterations as a biomarker for discrimination among RCC subtypes, specifically between chromophobe RCC and oncocytoma.

MATERIALS AND METHODS

1. Biological Samples

One hundred and twenty renal cell tumor samples comprising 30 cases of each of the four major subtypes (Clear Cell RCC, Papillary RCC, Chromophobe RCC, and Oncocytoma) were included in this study. These samples were consecutively selected from a larger series of patients diagnosed and treated at the Portuguese Oncology Institute – Porto, Portugal, who underwent partial or total nephrectomy, after informed consent. A small tumor sample was immediately snap-frozen, stored at -80ºC, and subsequently cut in a cryostat for nucleic acid (DNA and RNA) extraction. The bulk material was routinely fixed in buffered formalin and paraffin-embedded. The corresponding hematoxylin-eosin-stained sections were examined by a pathologist to determine the tumor type (Eble *et al.*, 2004), grade classification (Fuhrman *et al.*, 1982), and pathological stage according to the TNM staging system (Edge *et al.*, 2010). A representative paraffin block of each tumor was further chosen for immunohistochemical and FISH analyses.

For control purposes, four normal renal tissue samples, obtained from autopsies of patients without renal tumor were also selected. These were identified as normal kidney (NK) samples.

Relevant clinical data was collected from patient's clinical records.

To serve as a putative positive control for *PAX2* promoter methylation in tissue samples (Wu *et al.*, 2005), five samples of formalin-fixed, paraffin-embedded normal endometrium, collected from women submitted to hysterectomy for uterine leiomyomas, were also randomly selected for this study.

These studies were approved by the institutional review board (Comissão de Ética) of Portuguese Oncology Institute – Porto.

2. Methods

2.1 Assessment of PAX2 protein expression

2.1.1 Immunohistochemistry

Immunohistochemistry was performed according to the avidin-biotin method using the VECTASTAIN® Universal Elite ABC Kit [©Vector Laboratories, Burlingame, CA, USA].

Four micron-thick sections from the representative paraffin block of each renal cell tumor and of the five normal endometrium samples were placed in StarFrost® Adhesive slides [Knittel-Gläser, Germany]. The slides were deparaffinized with xylene and rehydrated with 100%, 90% and 70% ethanol solutions, and subsequently steamed in a 1x sodium citrate buffer solution [©Vector Laboratories, Burlingame, CA, USA] for 20 minutes in a 700 W microwave oven for antigen retrieval. Every 5 minutes, cool distilled water was added to avoid tissue detachment. At the end of this process, slides were cooled for 10 minutes in cool distilled water. Endogenous peroxidase was blocked by incubating the slides in a 0.6 % H_2O_2 solution for 20 minutes. After washing the slides in distilled water and PBS (Phosphate Buffered Saline)/tween 20 solution they were incubated with Normal Horse Serum 1:100 in PBS-Bovine Serum Albumin (BSA) for 30 minutes, in a humid chamber, at room temperature, to avoid antibody unspecific links. Then, the slides were incubated with the primary antibody for 18 hours, at 4º C, in a humid chamber. A rabbit monoclonal PAX2 antibody [Abcam, UK] was used in a 1:3000 dilution. The slides were next incubated with the biotynilated secondary antibody 1:100 in PBS/BSA for 30 minutes in a humid chamber, at room temperature.

Localization was performed by the standard avidin-biotin-immunoperoxidase method, by incubating the sections with the ABC complex 1:100 in PBS/BSA for 45 minutes, in a humid chamber, at room temperature. The slides were then immersed in a 3.3'-diaminobenzidine solution for 7 minutes, which functioned as the chromogen. After washing the slides in tap water they were counterstained with hematoxylin for 10 seconds and once again washed in tap water.

Finally, the sections were dehydrated using increasing ethanol concentrations (70%, 90% and 100%) and xylene, and the slides were mounted with Entellan® [Merck, Germany].

An unrelated clear cell RCC section showing intense immunoreactivity for PAX2 protein, was used as positive control. The negative control consisted on the omission of the primary antibody.

2.1.2 Scoring of immunohistochemistry staining

Following a low-magnification screening of the whole slide, multiple (generally 15 to 20) high-magnification microscopic fields were examined in each case to asses PAX2 expression. The immunoreactivity of nuclei from cells of the distal tubule and of the collecting duct of normal renal tissue adjacent to each tumor was used as internal positive control. The results of PAX2 expression in each tumor were expressed in a semiquantitative way according to the estimated percentage of positive tumor cells. Immunostaining of more than 10% of the tumor cell nuclei was required for scoring a case as positive. The positive cases were further divided in two categories according to the proportion of positive cells (Table 2). These criteria have been previously used by other researchers (Mazal *et al.*, 2005; Memeo *et al.*, 2007; Gupta *et al.*, 2009)

Table 2: Scoring of immunohistochemistry staining results.

Proportion of positive cells		Score
≤ 10%	Negative	0
>10% - 50%	Positive	1
> 50%		2

2.2 Nucleic acid extraction and quantification

2.2.1 DNA from renal tissues

DNA from RCT and NK samples was extracted by the phenol-chloroform method, at pH 8, as previously described (Pearson and Stirling, 2003). Briefly, the samples were digested by adding 2700 µL of buffer solution SE (75 mM NaCl; 25 mM EDTA), 300 µL of sodium dodecyl sulfate (SDS) 10% and 25 µL of proteinase K, 20 mg/mL [Sigma-Aldrich®, Germany] to each tissue sample, which were then placed in a bath at 55ºC, and incubated overnight. If necessary, the incubation went on for two or three additional days, and more proteinase K was added every day. After digestion, extraction was performed with phenol/chloroform [Sigma-Aldrich®, Germany; Merck, Germany] in Phase Lock

Gel™ Light tubes [5Prime, Germany]. The digested samples were transferred to these tubes containing the phenol/chloroform mixture and centrifuged for 20 minutes at 4000 rpm. Then, the upper aqueous phase was transferred to a new tube and the DNA precipitation followed with 6 mL of 100% cold ethanol and 1 mL of ammonium acetate 7.5 M [Sigma-Aldrich®, Germany]. Each sample was gently mixed and incubated overnight at -20ºC to improve DNA precipitation. Finally, the samples were washed twice with a 70% ethanol solution and then eluted in sterile distilled water [B. Braun, Melsungen, Germany].

DNA quality and concentration were analyzed in a spectrophotometer NanoDrop ND-1000 [NanoDrop Technologies, USA]. Eluted samples were stored at -20ºC.

2.2.2 RNA from the renal tissues

RNA from RCT and NK samples was extracted using the PureLink™ RNA Mini Kit [Invitrogen, CA, USA] according to the manufacturer's instructions. Briefly, 500 µL of *Lysis buffer* containing 1% of β-mercaptoethanol [Sigma-Aldrich®, Germany] were added to each sample and homogenized using a Rotor-stator homogenizer [VWR™, USA] for 45-90 seconds. An additional 500 µL of this solution were added to the samples. The samples were then centrifuged at 5000 rpm, at 4ºC for 5 minutes and the supernatant transferred into a new tube. Equal volume of ice cold 75% ethanol solution was added to the samples. The resulting mixture was vigorously shaked by hand and 700 µL of this solution were next transferred to a spin cartridge, which was previously placed in a collection tube. The tubes were centrifuged at 11000 rpm at room temperature, for 15 seconds. This process was repeated until all of the solution was processed. The samples were washed with 700 µL of *Wash Buffer I* and then with 500 µL of *Wash Buffer II*. This last washing step was repeated once. Then, the collection tube was discarded and the spin cartridge placed in a recovery tube. RNase-free water (2x 30 µL) was added to each spin cartridge and the tubes were centrifuged to allow for RNA elution.

RNA quantification and quality assessment were performed in a spectrophotometer NanoDrop ND-1000 [NanoDrop Technologies, USA]. RNA from each sample was also loaded on a 2% agarose gel to assess for integrity. Bands corresponding to both 18s and 28s rRNA should be visible in the agarose gel to consider the sample suitable for further analysis. The RNA samples were then stored at -80ºC.

2.2.3 DNA from formalin-fixed paraffin embedded normal endometrium tissues

DNA was extracted using the QIAamp® DNA FFPE Tissue Kit [QIAGEN, Germany] according to the manufacturer's instructions. Briefly, tissue sections were first deparaffinized and rehydrated using xylene and ethanol 100%. After this treatment, supernatant was removed by pippeting and samples were left to dry at room temperature until all residual ethanol was evaporated. The pellet was then ressuspended in 180 µL of *ATL Lysis Buffer* and 25 µL of proteinase K, and incubated at 55ºC overnight.

On the next day, samples were incubated for one hour at 90ºC to reverse formaldehyde modification of nucleic acids. After incubation, 200 µL of *AL Lysis Buffer* and 200 µL of 100% ethanol were added to the samples, and the samples were vortexed. The resulting lysate was transferred to the *QIAamp MinElute* column and the tubes were centrifuged at 8000 rpm for 1 minute. The column was then washed with 500 µL of *AW1 Wash Buffer* by centrifuging the tubes for 1 minute at 8000 rpm. The process was repeated with 500 µL of *AW2 Wash Buffer*. The column was placed in a recovery tube and 50 µL of warm water (heated at 90ºC) were added to the column to elute the DNA. After 5 minutes of incubation the tubes were centrifuged at 14000 rpm for 5 minutes. DNA quantification and quality assessment were performed as previously described for renal tissues. Samples were stored at -20ºC.

2.3 Assessment of *PAX2* mRNA expression

Quantitative reverse-transcription (qRT)-PCR was performed to assess *PAX2* expression. First, the extracted RNA was transcribed into cDNA which was then used as template for the PCR reaction.

The housekeeping gene hypoxanthine phosphoribosyltransferase 1 (*HPRT1*) was used as an endogenous control, to normalize for the input of template cDNA.

Quantitative expression of both endogenous control and target genes was determined using Taqman® Gene Expression Assays [Applied Biosystems, CA, USA].

2.3.1 cDNA synthesis from the extracted RNA

cDNA was synthesized by reverse transcription using the RevertAid™ H Minus First Strand cDNA synthesis Kit [Fermentas, Ontario, USA], according to the manufacturer's instructions. Briefly, 1 µL of Random hexamer was added to 500 ng of template RNA. This mixture was incubated at 70ºC for 5 minutes to allow for RNA denaturation. The

following components were then added: 2 µL of 5x Reaction Buffer, 0.5 µL of Ribolock RNase inhibitor (20 U/ µL) and 1 µL of 10 mM dNTP mix, and the samples were incubated at 25ºC for 5 minutes. Finally, 0.5 µL of RevertAid^{TM} H Minus M-MuLV Reverse Transcriptase (200 U/ µL) were added and reacted under the following conditions: 25ºC for 10 minutes, 42ºC for 60 minutes and 70ºC for 10 minutes.

The newly synthesized cDNA samples were eluted in 100 µL of DEPC water [MP Biomedicals, OH, USA] and stored at -20ºC.

2.3.2 Quantitative PAX2 expression analysis

Quantitative *PAX2* expression analysis was performed using Taqman® technology. The Taqman® assays are based on the FRET (Förster/Fluorescence Resonance Energy Transfer) technology and use a fluorogenic probe to enable detection as DNA copies accumulate during PCR cycles. TaqMan® probes consist of a fluorophore covalently attached to the 5'-end of the oligonucleotide probe and a quencher at the 3'-end. During amplification, the *Taq* polymerase cleaves the reporter from the probe, owing to its 5'-3' exonuclease activity, releasing it from the quencher and promoting its detection.

In this study, two Taqman® Gene Expression Assays were used. These are pre-designed optimized real-time PCR assays for gene expression quantification:

- For *HPRT1*, a Gene Expression Assay specific for *HPRT1* exons 6 and 7 (Hs 99999909_m1, [Applied Biosystems, CA, USA]) was used.

- For *PAX2*, a Gene Expression Assay specific for exons 1 and 2 (Hs01057413_m1, [Applied Biosystems, CA, USA]) was used.

The reactions were carried out in 96-well plates on an Applied Biosystems 7500 Real-time PCR system [Applied Biosystems, CA, USA], using the following conditions: 50 ºC for 2 minutes, 95 ºC for 10 minutes and 45 amplification cycles at 95 ºC for 15 seconds and 60 ºC for 1 minute.

In each reaction, 9 µL of cDNA, 1 µL of Taqman® Gene Expression Assay and 11 µL of Taqman® Gene Expression Assay Master Mix [Applied Biossystems, CA, USA] were used. All samples were run in triplicate. Two negative controls, consisting on the replacement of cDNA with DEPC-treated water [MP Biomedicals, OH, USA], were included in each plate.

The standard curve method was used for quantitation. This curve was built with a series of cDNA dilutions prepared from commercial Stratagene® QPCR Human Reference

total RNA [Agilent Technologies, Stratagene, CA, USA] or from a *PAX2* expressing renal cell tumor (oncocytoma), for *HPRT1* and *PAX2* analysis, respectively. *PAX2* expression levels were calculated by dividing the values of *PAX2* by those of the respective endogenous control values (*HPRT1*), obtained from qRT-PCR (mean quantity). This ratio was then multiplied by 1000 for easier tabulation.

2.4 Methylation analysis

Methylation analysis was performed using the methylation-specific PCR (MSP) method. This is a simple, sensitive and rapid method to determine the methylation patterns from small samples of DNA, allowing for the distinction between methylated and unmethylated alleles. This method requires testing with two pairs of primers which amplify methylated or unmethylated gene sequences in previously bisulfite-modified DNA.

2.4.1 Bisulfite modification of genomic DNA

All DNA samples (from RCTs, NKs and normal endometrium) were subjected to sodium bisulfite modification. This method allows for the subsequent evaluation of the methylation status of individual CpG dinucleotides in genomic DNA. During this reaction, the bisulfite converts all cytosine residues to uracil residues, excepting those that are methylated (5-mC). These methylated cytosine residues are resistant to the modification and remain unchanged. This method implies sulfonation and deamination of cytosines, converting them to uracil sulfonate. A subsequent desulfonation is necessary to complete the conversion into uracil. Bisulfite modification was performed using the EZ DNA Methylation-Gold™ Kit [Zymo Research, Orange, CA, USA] according to the manufacturer's instructions. Briefly, 1 µg of genomic DNA from each sample in a total of 20 µL was mixed with 130 µL of *CT conversion reagent* and then reacted under the following conditions: 98 ^{o}C for 10 minutes and 64 ^{o}C for 150 minutes. This mixture was then mixed with 600 µL of *M-binding buffer* already placed in a Zymo-Spin IC^{TM} cartridge and centrifuged at 10000 rpm for 30 seconds. The spin cartridge was washed with 100 µL of *M-Wash buffer* and centrifuged once again at 10000 rpm for 30 seconds. Subsequently, the samples were incubated with 200 µL of *M-Desulphonation Buffer* for 20 minutes at room temperature, to allow the removal of desulphonation residuals. The spin cartridge was then centrifuged at 10000 rpm for 30 seconds and two more washes with 200 µL *M-Wash buffer* were performed. Finally, the spin cartridge was placed in a recovery tube and

the samples were eluted in 30 + 30 µL of distilled water [B. Braun, Melsungen, Germany]. Eluted samples were stored at -50ºC.

2.4.2 Methylation analysis of PAX2 promoter

Bisulfite-modified genomic DNA was tested using two sets of primers, each recognizing either the methylated or the unmethylated sequences located in the promoter region of the *PAX2* gene. Two adjacent regions were screened to assess the promoter methylation status. Primer sequences are summarized in Table 3, along with amplicon lengths and positions, and optimized annealing temperatures. Primers were provided by Metabion, Germany.

Table 3: Sequences of the primers used in the methylation-specific PCR experiments, amplicons size (**AS**), amplicons location in relation to the transcriptional start site (**AL**), and optimized annealing temperatures (**AnT**).

Primer	Primer sequence (5' – 3')	AS (bp)	AL	AnT (ºC)	Reference
PAX2_M (F1)	GGGTTTTTTTCGTCGAAGTTC	170	-676 to -846	60	(Wu *et al.*, 2005)
PAX2_M (R1)	ACTAAAACCTCGACTCCCGAT				
PAX2_U (F1)	GGTTTTTTTTGTTGAAGTTTGG	172	-673 to -845	62	(Wu *et al.*, 2005)
PAX2_U (R1)	AAAACTAAAACCTCAACTCCCAAT				
PAX2_M (F2)	AGTTGTTAGCGTCGTTCGGTTT	139	-489 to -628	62	(Metsuyanim *et al.*, 2008)
PAX2_M (R2)	ACAATCCCGAAAATATCCGAAATAA				
PAX2_U (F2)	AGAGTTGTTAGTGTTGTTTGGT	141	-489 to -630	59	-
PAX2_U (R2)	ACAATCCCAAAAATATCCAAAAT				

M - Methylated**, U –** Unmethylated**, F** – Forward; **R** – Reverse; **bp** – base pairs

The PCR reactions were performed in an Applied Biosystems Veriti® Thermal Cycler [Applied Biosystems, CA, USA]. Each PCR tube contained 14.36 µL of sterile distilled water [B. Braun, Melsungen, Germany], 2 µL of 10x DyNAzyme™ Hot Start Reaction Buffer [Finnzymes, Finland], 0.2 mM of dNTPs [Fermentas, Ontario, Canada], 250 nM of primer forward and 250 nM of reverse primer, 0.24 µL of DyNAzyme™ II Hot

Start DNA polymerase 2U/µL [Finnzymes, Finland], and 2 µL of sample DNA, to a final volume of 20 µL.

The PCR amplifications were performed as follows: ten-minute 94ºC incubation was followed by 38 cycles of 30 seconds at 94ºC, 30 seconds at annealing temperature (see Table 3) and 30 seconds at 72ºC. A ten-minute elongation step at 72ºC completed the PCR amplification. The PCR products were then separated on a 2% agarose gel.

Primers specificity was assessed using CpGenome™ Universal Methylated DNA [Millipore, CA, USA] and CpGenome ™ Universal Unmethylated DNA [Millipore, CA, USA] as positive and negative controls, respectively.

2.5 Fluorescent *in situ* hybridization analysis

The aim of this technique is to identify either imbalances in the form of gains or losses of chromosome segments, or to detect specific breakpoints with or without imbalances. Thus, it can be defined as the morphological localization of genetic sequences, by determining the presence or absence of specific RNA or DNA species. The identification of these sequences is based on the property of nucleic acids to anneal to one another in a specific manner to form hybrids. Therefore, by labeling one of these strands, the hybrids can be detected by several means, including fluorescent methods.

The basic requirements of this technique are therefore: a probe that is specific for the sequence of interest, fluorescent labeling of this probe to allow detection and a biological specimen with preservation of sufficient morphological detail to determine the localization of the labeled probe after hybridization (Kjeldsen and Kølvraa, 2002).

For this particular study, Bacterial Artificial Chromosome (BAC) clones targeting the *PAX2* gene (RP11_1061B5) were selected using the UCSC Human Genome Browser and obtained from the BACPAC Resources Center [Oakland, USA]. The extracted plasmid DNA containing an insert complementary to the target sequence was subsequently labeled with a fluorochrome and then used as a probe to perform FISH analysis.

2.5.1 Bacteria growth

The *E. coli* bacteria were first grown in LB (Luria-Bertani broth) agarose medium, supplemented with cloramphenicol 12.5 mg/mL, overnight at 37ºC. On the next day, an individual colony was inoculated in 10 mL of liquid LB medium and incubated at 37ºC, for 16 hours with vigorous agitation.

The tube containing the *E.coli* LB culture was then centrifuged at 4000 rpm for 30 minutes. The supernatant was discarded and the pellet used for plasmid DNA extraction.

2.5.2 Plasmid DNA isolation

Plasmid DNA was extracted using the NucleoSpin® Plasmid [Macherey-Nagel, Germany], according to manufacturer's instructions. Briefly, the first step consisted in resuspending the cell pellet using 250 µL of *Buffer A1*. Then 250 µL of lysis *Buffer A2* were added and mixed gently with the sample, and incubated for up to 5 minutes at room temperature. Next, 300 µL of neutralization *Buffer A3* were added and mixed gently by inverting the tube. The sample was subsequently centrifuged for 12 minutes at 10500 rpm at room temperature, to clarify the lysate. The resulting supernatant was placed in a NucleoSpin® Plasmid column and centrifuged at 10500 rpm for 1 minute. The flow-through was discarded and 600 µL of wash *Buffer A4* were added to the column which was centrifuged at 10500 rpm for 1 minute. The column was once again centrifuged at 10500 rpm for 2 minutes to dry the silica membrane. Next, the column was placed in a new tube and 60 µL of elution *Buffer AE* were added, and incubated for 1 minute at room temperature to elute the DNA. Finally, the column was centrifuged at 10500 rpm for 1 minute and DNA quality and concentration were analyzed in a NanoDrop ND-1000 spectrophotometer [NanoDrop Technologies, USA].

2.5.3 Plasmid DNA amplification

Plasmid DNA was amplified before labeling to produce more copies of the sequence targeting the gene of interest.

The plasmid DNA concentration was adjusted to 10 ng/µL to allow amplification using the Illustra GenomiPhi V2 DNA Amplification Kit [GE Healthcare, US]. Briefly, 1 µL of template DNA was mixed with 9 µL of *Sample Buffer*. The template DNA was then denatured by heating the sample at 95 ºC for 3 minutes. Next, 9 µL of *Reaction Buffer* and 1 µL of *Enzyme Mix* were added to the sample, and the mixture was placed in a thermocycler under the following conditions: 16 cycles at 30 ºC for 60 minutes, and 65 ºC for 10 minutes. The samples were stored at -20ºC.

2.5.4 Nick translation reaction

Labeling of probes was performed using an enzymatic method called nick-translation. This reaction employs two enzymes, deoxyribonuclease I (DNaseI) and DNA polymerase I. The DNase I hydrolyses nicks in each strand of the DNA molecule at random, and DNA polymerase removes individual base pairs from the nick in the 5' to 3' direction (exonuclease function), adds new nucleotides from the 3' nick copying the template in the opposite DNA strand (polymerase function) and has also a 3' to 5' proof-reading activity. In this way, labeled nucleotides are incorporated into the newly synthesized DNA (Schwarzacher and Heslop-Harrison, 2000).

The nick translation reaction was performed as follows. Firstly, 1.5 µL of the amplified DNA was mixed with 30 µL of sterile bi-distilled water [B. Braun, Melsungen, Germany] and heated at 90ºC for 5 minutes to allow DNA denaturation. Then, 5 µL of nucleotide mix, 1.5 µL of Spectrum Green-dUTP [Enzo Life Sciences, USA], 1 µL of Polymerase I [Invitrogen, CA, USA], 10 µL of Polymerase I/DNase [Invitrogen, CA, USA] and 1 µL of $MgCl_2$ [Sigma-Aldrich®, Germany] were added to the diluted DNA. This mixture was incubated in a thermocycler at 15ºC for 45 minutes and then at 70ºC for 15 minutes, to allow the enzymes to function properly.

At the end of this incubation the DNA was precipitated using 7.5 µL of sodium acetate, and 140 µL of 100% ethanol. Fifteen µL of Human Cot DNA [Invitrogen, CA, USA] were also added to avoid unspecific probe hybridization. The products were placed at -20ºC overnight to improve DNA precipitation.

On the next day, samples were centrifuged at 14000 rpm for 30 minutes, then the supernatant was eliminated and the pellet was dried for 1 hour in the dark. The DNA was finally eluted in 10 µL of Vysis LSI/WCP Hybridization Buffer [Abbott Molecular, Illinois, USA] and mixed with 1 µL of a Vysis centromeric probe for chromosome 10, labelled with SpectrumOrange [Abbott Molecular, Illinois, USA]. These probes were stored at -20ºC.

Adequate mapping and probe specificity was confirmed by hybridization onto normal human metaphases.

2.5.5 Sample processing

The thirty chromophobe RCC samples were tested.

Four-micron thick sections from formalin-fixed, paraffin-embedded tissues, placed in StarFrost® Adhesive slides (Knittel-Gläser, Germany) were first deparaffinized in two series of xylene followed by two series of 100% ethanol, and then rinsed in a 2x SSC [Vysis, Downers Grove, IL, USA] buffer solution twice, for 2 minutes each. The slides were then placed in a sodium thiocyanate (NaSCN) [Sigma-Aldrich, Germany] solution, for 15 minutes at 80ºC and rinsed once again in a 2x SSC buffer solution. The tissue was digested with 100 µL of a 4mg/mL pepsin solution for 6 minutes at 37ºC. After this incubation step, the slides were rinsed in a 2x SSC buffer solution and then dehydrated with increasing ethanol concentrations and dried at room temperature before staining.

The sections were incubated with a mixture of the two probes, including the one designed to hybridize with the *PAX2* gene, labeled with SpectrumGreen, and a centromeric probe for chromosome 10, labeled with SpectrumOrange [Vysis, Abbott Laboratories, Illinois, USA], and placed in a ThermoBrite® Denaturation/Hybridization System [Abbott Molecular, Illinois, USA], for 8 minutes at 80ºC and 18 hours at 37ºC, to allow co-denaturation and probe hybridization, respectively. Following this hybridization, slides were washed in a 2x SSC/0.5% Igepal [Sigma-Aldrich, Germany] solution, at 73ºC for 5 minutes and then in a 2x SSC/0.1% Igepal solution at room temperature for 3 minutes.

Slides were counterstained with *Vectashield Mounting Medium for Fluorescence with DAPI* (4',6-diamidino-2-phenylindole) [Vector Laboratories, Burlingame, CA, USA] and fluorescent images corresponding to DAPI, SpectrumGreen and SpectrumOrange were sequentially captured with a Cohu 4900 CCD camera, with the use of an automated filter wheel coupled to a Zeiss Axioplan fluorescence microscope [Zeiss, Oberkochen, Germany] and a CytoVision system version 2.7 [Applied Imaging, Santa Clara, CA, USA].

2.5.6 FISH scoring

For scoring purposes, only intact, non-overlapping nuclei were considered. An abnormal population was considered representative when at least 10% of the neoplastic cell nuclei presented a copy number change.

2.6 Statistical analysis

The chi-square test or Fisher's exact test were used to seek for differences in the frequency of immunoreactivity for PAX2 protein according to the immunohistochemical scoring, among the four renal cell tumor types. These tests were also used to search for differences in the frequencies of immunoreactivity for PAX2 protein among the different pathological tumor stages and Fuhrman grades. Moreover, the directional measure Somers'd was computed. Somers'd statistics varies from -1 to 1 and assesses the association between two ordinal variables. Values near 1 reveal a strong positive association, whereas values near -1 reveal a strong negative association.

To assess the value of PAX2 protein immunohistochemical expression for the discrimination of chromophobe RCC from oncocytoma, the sensitivity, specificity, positive and negative predictive values (PPV and NPV) were determined using the 10% or the 50% cutoff values.

The median and the interquartile range of *PAX2* mRNA expression levels for each subtype of renal cell tumor were determined. Differences among the four groups were assessed by the Kruskal-Wallis non-parametric test, followed by pairwise comparisons (ccRCC vs. chrRCC; pRCC vs. chrRCC; oncocytoma vs. chrRCC; ccRCC vs. pRCC; ccRCC vs oncocytoma; pRCC vs. oncocytoma) using the Mann-Whitney U test, when appropriate. The association between between *PAX2* mRNA expression levels and the protein expression (immunohistochemistry score) was carried out using the Mann-Whitney test.

The relationship between *PAX2* mRNA expression levels and clinicopathological variables, such as tumor grade and stage, were evaluated using the Kruskal-Wallis test, followed by a Mann-Whitney U test, whereas the correlation between *PAX2* expression levels and patients' age was assessed by the Spearman non-parametric correlation test.

The relationship between FISH findings and immunoexpression results for chrRCC was assessed by a chi-square or Fisher's exact test, and the directional measure Somers'd was also computed. Moreover, the association between FISH findings and *PAX2* mRNA levels for chrRCC was estimated using the Kruskal-Wallis test.

The level of significance was set at $p < 0.05$ and the Bonferroni's correction was used when appropriate. All tests were two-sided.

Statistical analysis was performed with SPSS for Windows, version 15.0 [SPSS, Chicago, IL, USA].

RESULTS

1. Clinicopathological data

Relevant clinical and pathological features of the patients included in this study are summarized in Table 4. Although this is not a consecutive but a selective series of patients, males were more frequently diagnosed with renal cell tumor and the median age at diagnosis was 59 years.

Table 4: Clinical and pathological features of patient population.

Clinicopathological features	RCT
Patients, n	120
Gender, n (%)	
Male	70 (58)
Female	50 (42)
Median age, yrs (range)	59 (29 - 83)
Pathological stage*, n (%)	
I	50 (56)
II	22 (24)
III	16 (18)
IV	2 (2)
Furhman grade*, n (%)	
1	2 (2)
2	29 (32)
3	39 (44)
4	20 (22)

*Includes RCC cases only.

2. PAX2 expression

2.1 Protein expression

To characterize PAX2 protein expression in renal cell tumors, immunohistochemical analysis was performed. As expected, immunoreactivity for PAX2 was found in cell nuclei only.

In general, normal renal tissue did not show immunoreactivity for PAX2, with the exception of distal tubules and collecting duct cells which presented intense and homogeneous staining (Figure 12, **A**).

Concerning tumor cells, staining was more intense in ccRCC and oncocytomas, as well as in pRCC type 1 (Figure 12, **B**, **F** and **C**). The vast majority of ccRCC and oncocytoma were considered positive, whereas most of chrRCC were negative (Figure 12, **E**). Concerning pRCC, positive cases were slightly more prevalent. The results of immunostaining scoring for PAX2 are summarized in Table 5.

Concerning normal endometrium samples, immunostaining was apparent in all nuclei of endometrial glands (Figure 12, **G**) of the tested cases (n= 5).

Table 5: Immunohistochemical expression of PAX2 in histologic sections of renal cell tumors.

	Negative, n (%)	**Positive, n (%)**	
RCT Subtype	≤10%	>10 – 50%	>50%
Clear cell	1 (3.3)	4 (13.4)	25 (83.3)
Papillary	13 (43.3)	4 (13.4)	13 (43.3)
Type 1	6 (60)	0 (0)	4 (40)
Type 2	7 (35)	4 (20)	9 (45)
Chromophobe	20 (66.7)	6 (20)	4 (13.3)
Oncocytoma	3 (10)	5 (16.7)	22 (73.3)

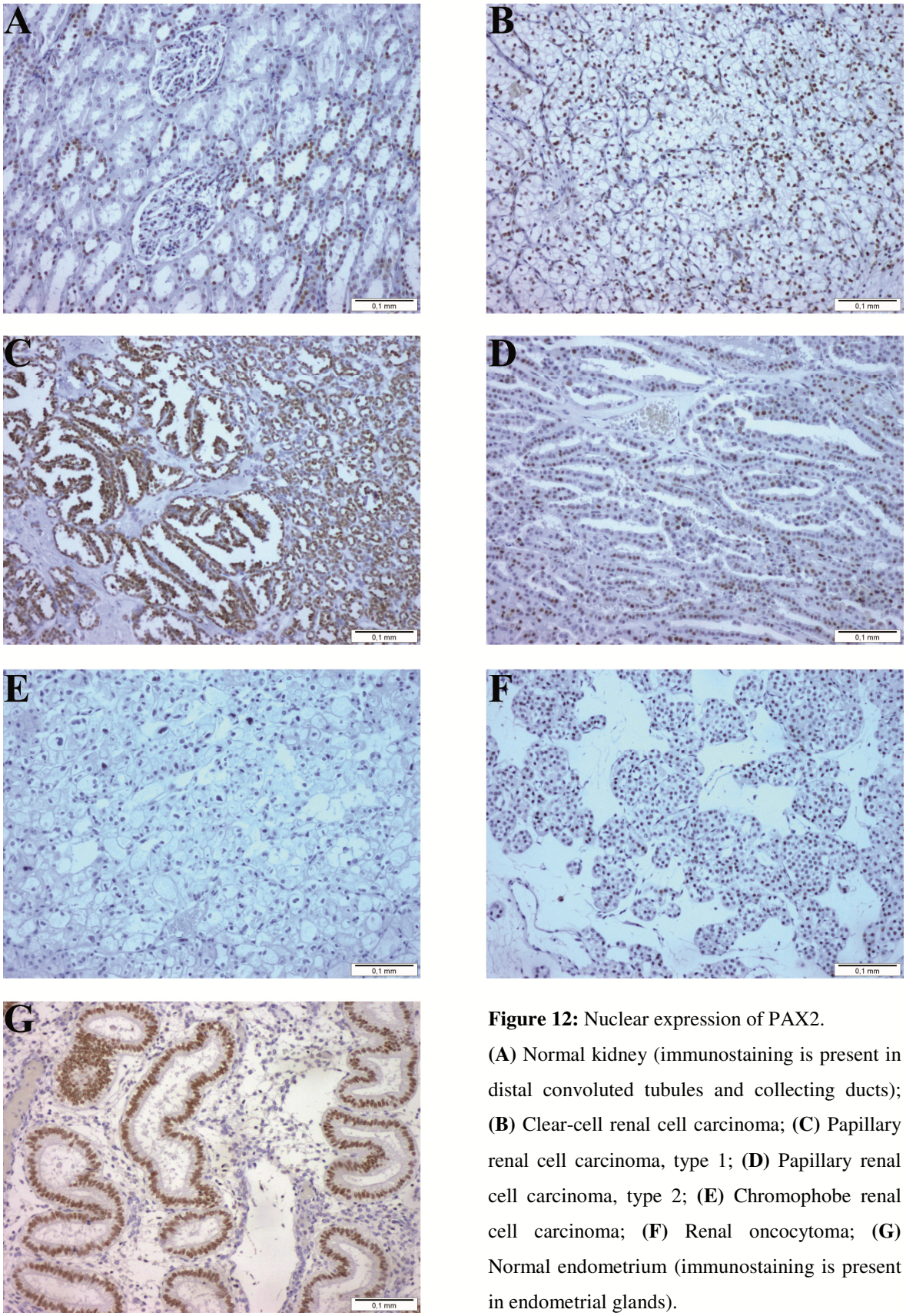

Figure 12: Nuclear expression of PAX2.
(A) Normal kidney (immunostaining is present in distal convoluted tubules and collecting ducts); **(B)** Clear-cell renal cell carcinoma; **(C)** Papillary renal cell carcinoma, type 1; **(D)** Papillary renal cell carcinoma, type 2; **(E)** Chromophobe renal cell carcinoma; **(F)** Renal oncocytoma; **(G)** Normal endometrium (immunostaining is present in endometrial glands).

The chi-square test detected significant differences in PAX2 expression among the four subtypes of renal cell tumors ($p < 0.001$). Pairwise comparisons disclosed significant differences in all cases ($p < 0.01$) except for pRCC *vs.* chrRCC ($p = 0.119$) and for oncocytoma *vs.* ccRCC ($p = 0.612$).

Moreover, no significant differences in PAX2 expression were found between type 1 and type 2 pRCC, using either the 10% ($p = 0.270$) or the 50% cutoff values ($p = 1$).

Because the morphological differential diagnosis between chrRCC and oncocytoma is sometimes troublesome, we tested whether PAX2 immunostaining might be used as an ancillary tool for histopathological assessment. We also determined the performance of PAX2 immunoexpression for discriminating chrRCC from oncocytoma in previously published studies. These results are summarized in the same table (Table 6).

Table 6: Performance of PAX2 immunoscoring for the discrimination between chromophobe RCC and oncocytoma, in this study and in previously published reports (**Se**: Sensitivity; **Sp**: Specificity; **PPV**: Positive predictive value; **NPV**: negative predictive value).

	Se (%)	**Sp (%)**	**PPV (%)**	**NPV (%)**
Present study				
10% cutoff	67	90	87	73
50% cutoff	87	73	76	85
Gupta *et al.* 2009				
10% cutoff	94	100	100	85
50% cutoff	94	65	89	79
Mazal *et al.* 2005				
10% cutoff	91	10	50	54
50% cutoff	100	3.5	51	100
Memeo *et al.* 2007				
10% cutoff	91	87	77	95

Concerning the clinicopathological data, we found significant differences between the immunoexpression frequencies according to pathological stage ($p = 0.03$) and Furhman

grade (p = 0.04). These results are shown in Table 7 and Table 8, respectively. Both stage and grade were grouped in 2 categories for statistical purposes.

Table 7: Correlation between PAX2 immunoexpression and pathological tumor stage, n (%).

	Immunoexpression scoring		**P**
	≤ 10%	**> 10%**	
Stages 1 & 2	23 (32%)	49 (68%)	0.03
Stages 3 & 4	11 (61%)	7 (39%)	

Table 8: Correlation between PAX2 immunoexpression and Furhman nuclear grade, n (%).

	Immunoexpression scoring		**P**
	≤ 10%	**> 10%**	
Grades 1 & 2	7 (23%)	24 (77%)	0.04
Grades 3 & 4	27 (46%)	32 (54%)	

Moreover, Somers'd directional measure revealed a slightly, though significant, negative association between the immunoexpression frequency and pathological tumor stages (d = -0.236, p = 0.031) or Furhman grades (d = -0.227, p = 0.021).

2.2 Quantitative mRNA expression

A quantitative analysis was performed to assess *PAX2* mRNA gene expression in the four renal cell tumor subtypes, and the results are displayed in Figure 13.

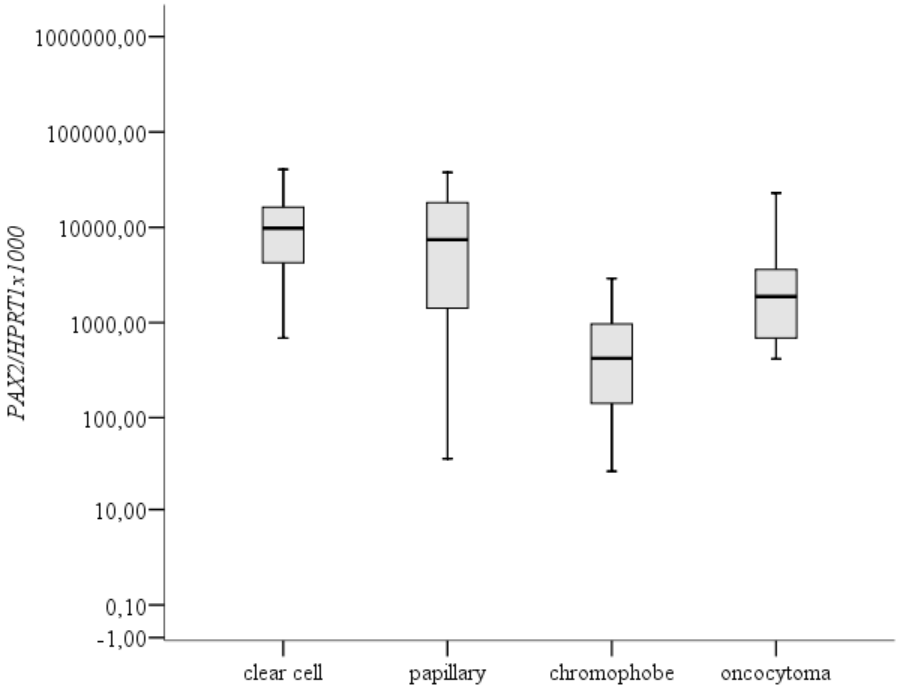

Figure 13: Boxplot of the relative mRNA expression levels (Log 10 transformed) of *PAX2* in clear cell RCC, papillary RCC, chromophobe RCC, and oncocytoma (n=120).

The distribution of *PAX2* mRNA expression levels according to the renal cell tumor subtype is displayed in Table 9. The Kruskal-Wallis test detected significant differences among the renal cell tumor subtypes ($p < 0.001$). Although *PAX2* mRNA expression levels did not differ between ccRCC and pRCC, both were significantly higher when compared to chrRCC and oncocytoma ($p < 0.001$, except for papillary *vs.* oncocytoma: $p = 0.011$). Moreover, mRNA expression levels in oncocytomas also differed significantly from those of chrRCC ($p < 0.001$).

Table 9: Distribution of *PAX2* mRNA expression levels [(PAX2/HPRT1) × 1000 expressed as median (interquartile range)] according to renal cell tumor subtype.

RCT Subtype	**mRNA expression** Median (interquartile range)
Clear cell	9598.6 (3717.0 – 16581.9)
Papillary	7464.8 (1390.2 – 18196.0)
Chromophobe	424.5 (135.2 – 974.8)
Oncocytoma	1942.7 (683.7 – 3815.5)

When *PAX2* mRNA expression levels were compared with PAX2 immunoexpression scoring, negative cases (≤10% immunostained nuclei) showed lower median mRNA levels than positive cases (>10% immunostained nuclei), and this difference was statistically significant (p = 0.011), as illustrated in Figure 14. When the 50% cutoff value was used the same trend was observed and the difference was once again statistically significant (p = 0.007).

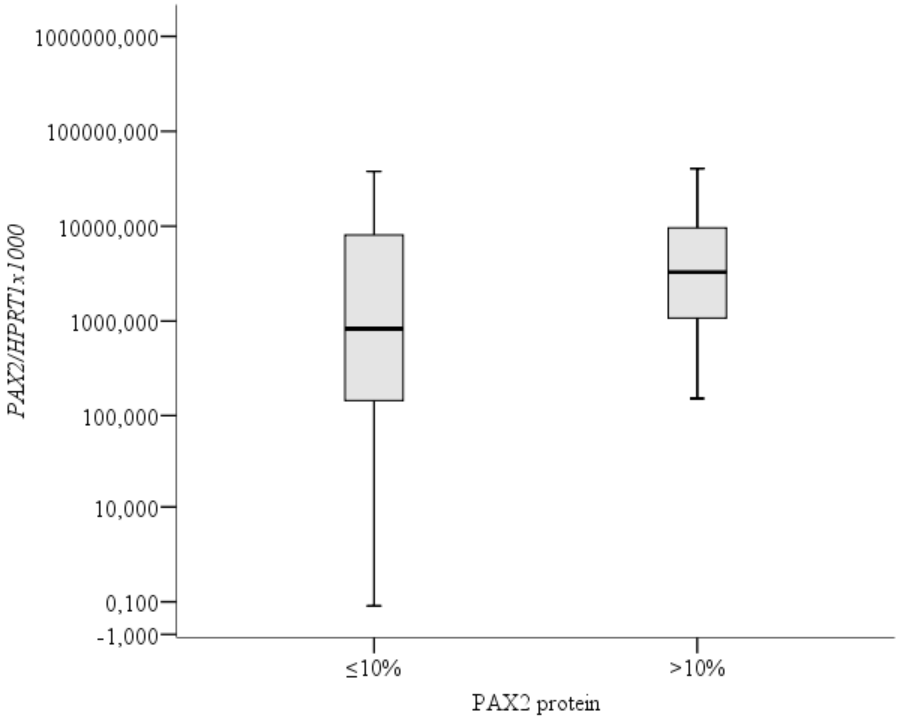

Figure 14: Boxplot of the distribution of *PAX2* mRNA expression levels (Log 10 transformed) according to PAX2 immunoexpression scoring using the 10% cutoff value (n=120).

No correlation was found between *PAX2* mRNA expression levels and patients' age (r= -0.112, p= 0.295) (Figure 15) or pathological tumor stage (p = 0.542) (Figure 16).

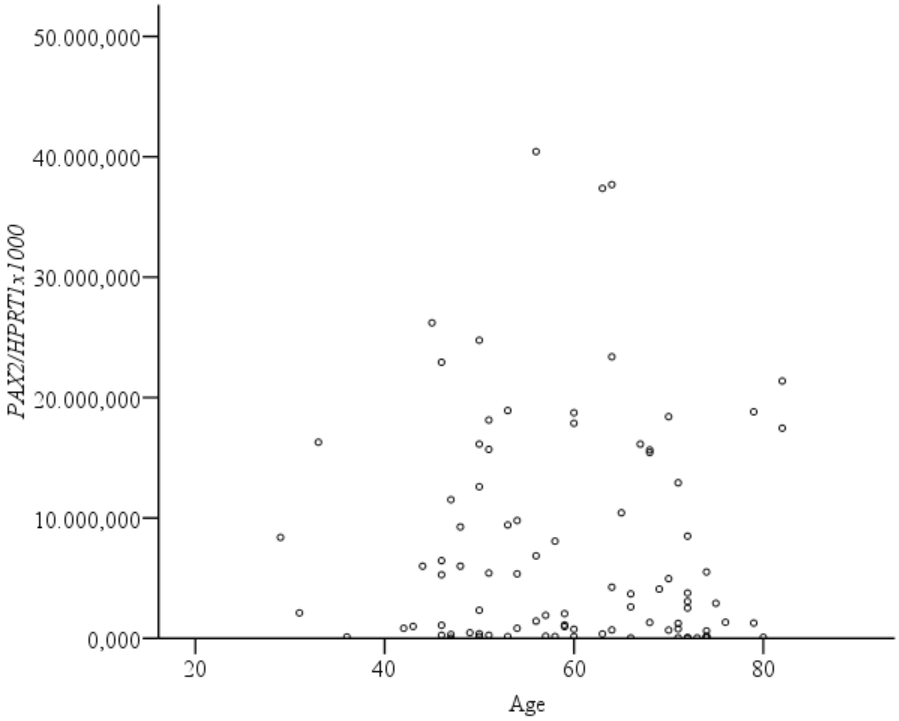

Figure 15: Scatterplot for the correlation between age and *PAX2* expression levels (n=120).

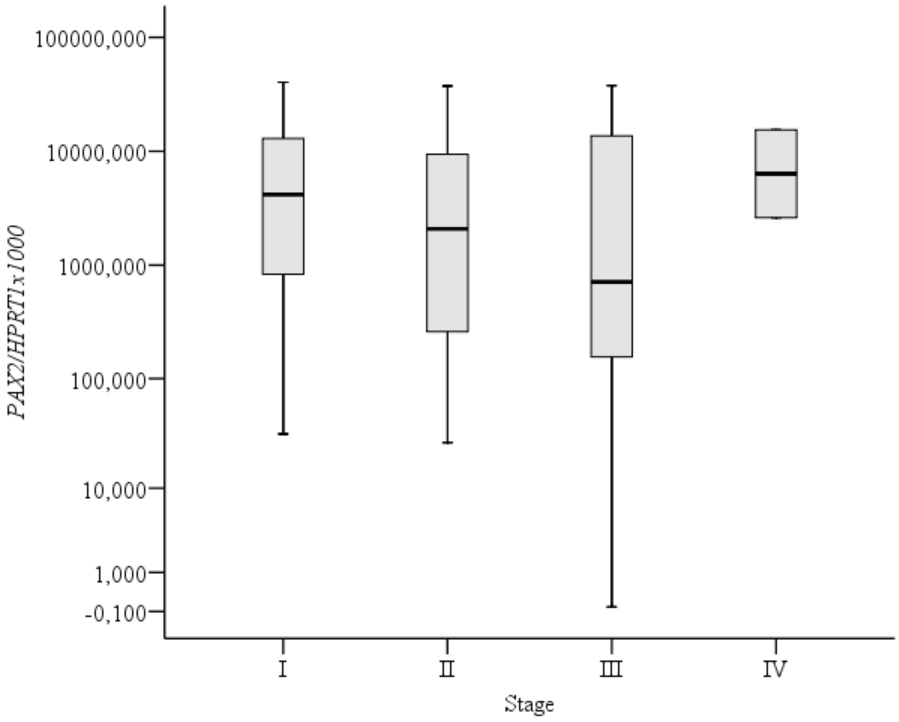

Figure 16: Boxplot of the *PAX2* mRNA expression levels (Log10 transformed) distribution according to the pathological stage (n = 90).

However, *PAX2* mRNA expression levels differed significantly among the Fuhrman grades ($p < 0.001$) (Figure 17). Grade 4 tumors displayed the lowest relative median levels and these statistically differed from those of grade 2 and grade 3 tumors ($p < 0.01$ for both).

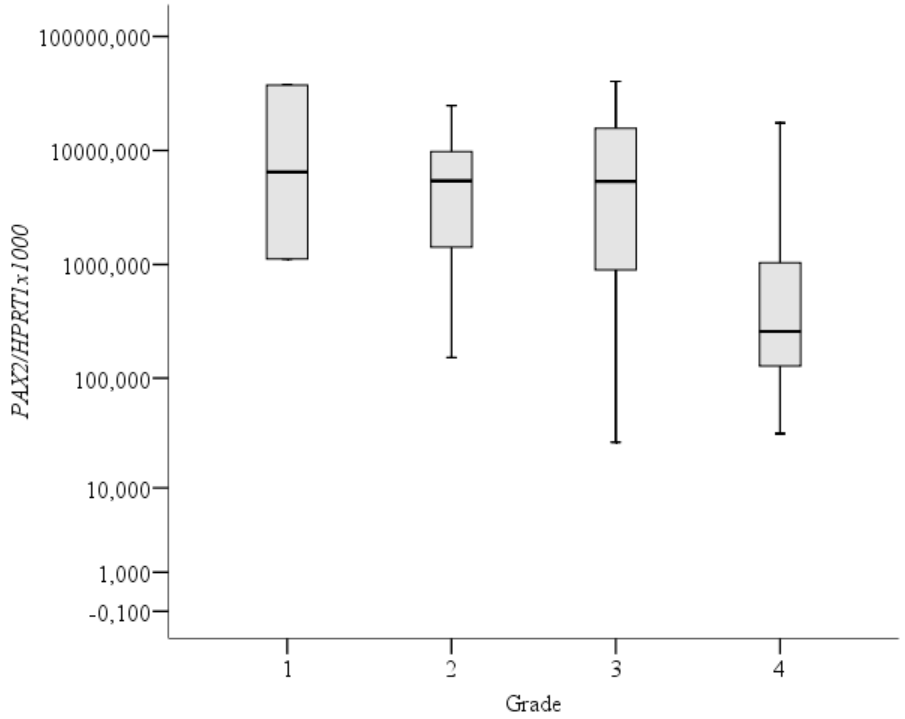

Figure 17: Boxplot of the *PAX2* mRNA expression levels (Log10 transformed) distribution according to the Fuhrman grading (n = 90).

3. *PAX2* promoter methylation assessment

The promoter methylation status was first assessed using primers specific for the promoter region spanning -676 to -846, in relation to the transcriptional start point, according to Wu *et al.* (Wu *et al.*, 2005). Methylation of CpG dinucleotides located in this region was not detected in any of the tumor (Figure 18) or normal (Figure 19) tissue samples.

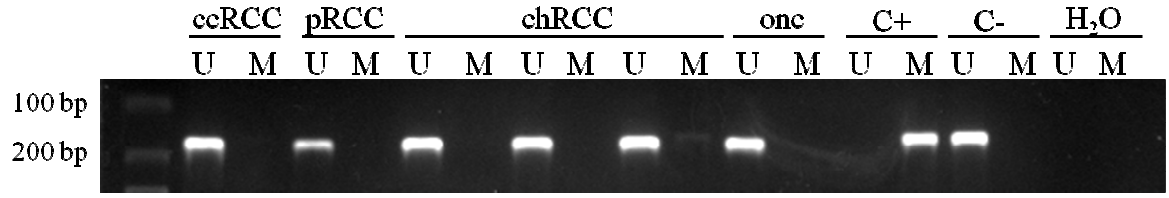

Figure 18: Representative methylation-specific PCR results from the analysis of *PAX2* promoter region (-676 to -846; primer set 1) in renal cell tumors. A visible PCR product in lanes U indicates the presence of unmethylated alleles whereas a PCR product in lanes M indicates the presence of methylated alleles. **C+**: fully methylated DNA, positive control for methylated samples; **C-**: fully unmethylated DNA, positive control for unmethylated samples; **H_2O**: negative control. **U**: lane for unmethylated MSP; **M**: lane for methylated MSP.

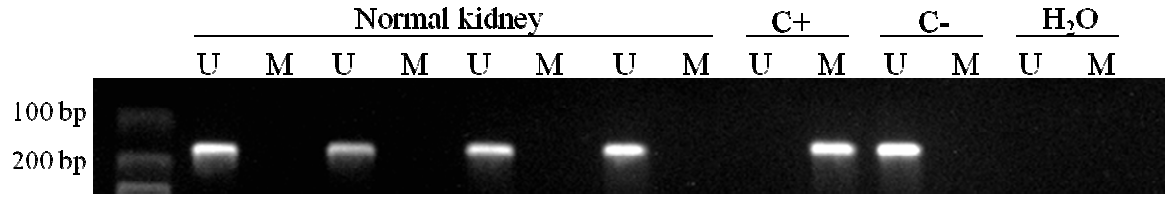

Figure 19: Representative methylation-specific PCR results from the analysis of *PAX2* promoter region (-676 to -846; primer set 1) in normal kidney tissues. A visible PCR product in lanes U indicates the presence of unmethylated alleles whereas a PCR product in lanes M indicates the presence of methylated alleles. **C+**: fully methylated DNA, positive control for methylated samples; **C-**: fully unmethylated DNA, positive control for unmethylated samples; **H_2O**: negative control. **U**: lane for unmethylated MSP; **M**: lane for methylated MSP.

These primers were also tested in DNA from normal endometrium as Wu and colleagues reported the presence of *PAX2* promoter methylation in this tissue using these same primer sequences (Wu *et al.*, 2005). As shown in Figure 20, all normal endometrium tissue samples tested were found to be unmethylated for *PAX2*.

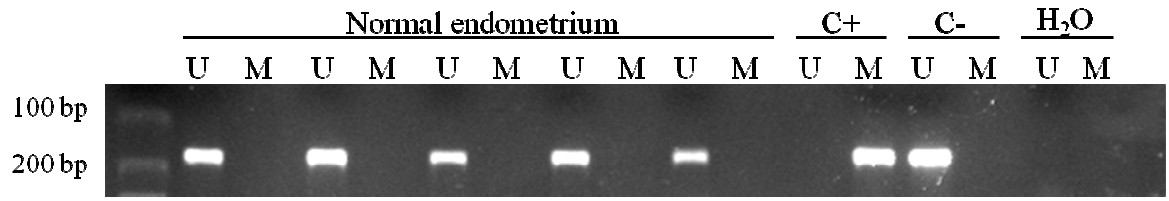

Figure 20: Representative methylation-specific PCR results from the analysis of *PAX2* promoter region (-676 to -846; primer set 1) in normal endometrium tissues. A visible PCR product in lanes U indicates the presence of unmethylated alleles whereas a PCR product in lanes M indicates the presence of methylated alleles. **C+**: fully methylated DNA, positive control for methylated samples; **C-**: fully unmethylated DNA, positive control for unmethylated samples; **H_2O**: negative control. **U**: lane for unmethylated MSP; **M**: lane for methylated MSP.

Because Metsuyanim *et al.*, 2008 reported *PAX2* methylation in a region downstream (-489 to -628 in relation to the transcriptional start site) of that analyzed by Wu *et al.*, we also used the set of primers published by the former researchers (Metsuyanim *et al.*, 2008) in our set of samples. However, no methylation was found neither in renal tumors (Figure 21) nor in normal renal tissues (Figure 22).

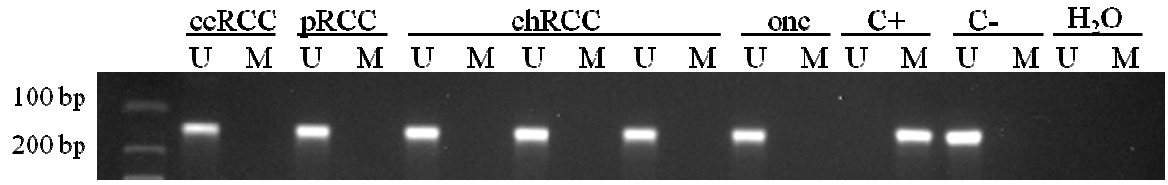

Figure 21: Representative methylation-specific PCR results from the analysis of *PAX2* promoter region (-489 to -628; primer set 2) in renal cell tumors. A visible PCR product in lanes U indicates the presence of unmethylated alleles whereas a PCR product in lanes M indicates the presence of methylated alleles. **C+**: fully methylated DNA, positive control for methylated samples; **C-**: fully unmethylated DNA, positive control for unmethylated samples; **H_2O**: negative control. **U**: lane for unmethylated MSP; **M**: lane for methylated MSP.

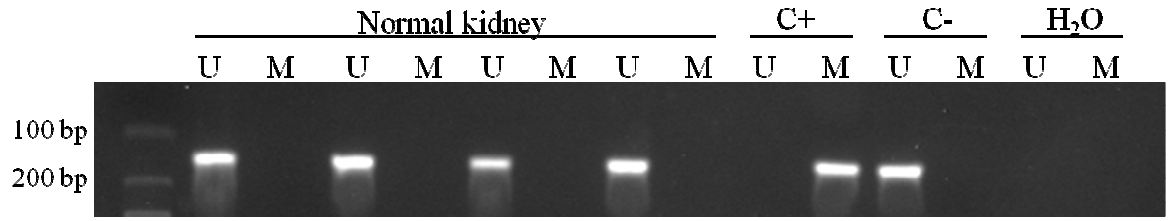

Figure 22: Representative methylation-specific PCR results from the analysis of *PAX2* promoter region (-489 to -628; primer set 2) in normal kidney tissues. A visible PCR product in lanes U indicates the presence of unmethylated alleles whereas a PCR product in lanes M indicates the presence of methylated alleles. **C+**: fully methylated DNA, positive control for methylated samples; **C-**: fully unmethylated DNA, positive control for unmethylated samples; **H_2O**: negative control. **U**: lane for unmethylated MSP; **M**: lane for methylated MSP.

4. FISH findings

All 30 chrRCC cases were tested for chromosome 10/*PAX2* copy number using a centromeric FISH probe targeting chromosome 10 and a probe targeting the *PAX2* gene, respectively. Four of these chrRCC samples were not technically analyzable (NA). From the remainder cases, chromosome 10 loss was seen in 18 (69%) tumors, whereas gain was seen in 2 (8%) chrRCC cases. No ch10/*PAX2* copy number change was observed in the remaining chrRCC cases. *PAX2* locus deletion alone was not found in any of the analyzed samples. Figure 23 shows representative FISH images from the analyzed chrRCC.

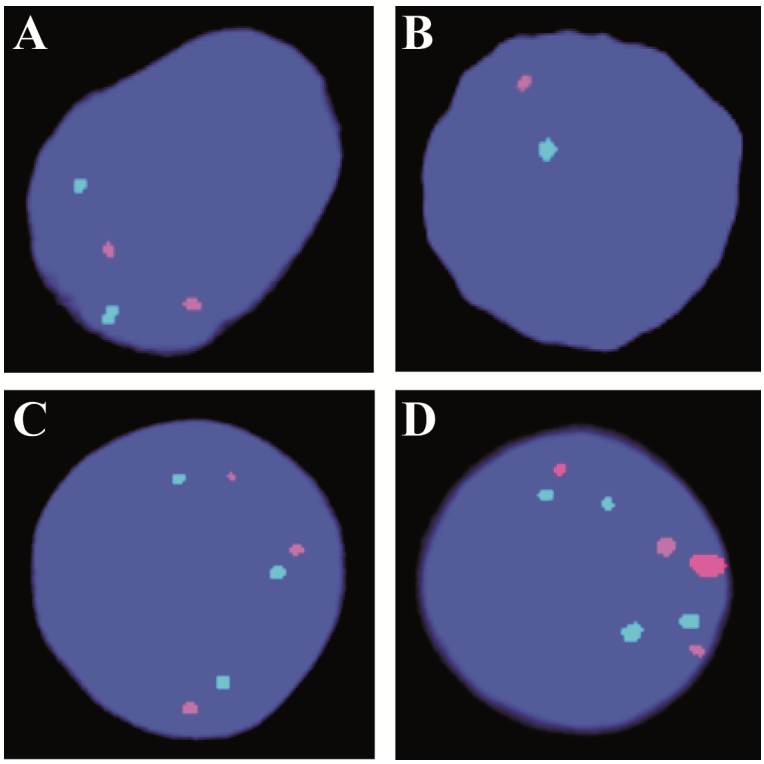

Figure 23: Representative FISH images from chromophobe RCC (chromosome 10 probe in red; *PAX2* probe in green). **(A)** Two copies of chromosome 10 centromere and two copies of *PAX2* (normal). **(B)** One copy of chromosome 10 centromere and one copy of *PAX2* (monosomy). **(C)** Three copies of chromosome 10 centromere and three copies of *PAX2* (trisomy). **(D)** Four copies of chromosome 10 centromere and four copies of *PAX2* (tetrasomy).

Table 10: FISH results for ch10/*PAX2* copy number and distribution of the immunoexpression frequencies and mRNA expression levels, in chrRCC cases.

FISH analysis	Immunoexpression, n (%)				mRNA expression Median (interquartile range)
	10% cutoff		50% cutoff		
	-	+	-	+	
Monosomy	17 (94)	1 (6)	18 (100)	0 (0)	213.2 (104.9 – 1000.4)
No ch10 loss	1 (17)	5 (83)	4 (67)	2 (33)	524.7 (114.1 – 1508.3)
Polysomy	0 (0)	2 (100)	1 (50)	1 (50)	384.7 and 527.7 *

* *Descriptive values*

Significant differences in PAX2 immunoexpression were observed among the three categories of ch10/*PAX2* copy number changes, when both the 10% ($p < 0.001$) and the 50% ($p = 0.018$) cutoff values were used (Table 10). Moreover, Somers'd directional measure revealed a strong positive association between the immunoexpression frequency and the ch10/*PAX2* copy number changes, for both 10% ($d = 0.8$, $p < 0.001$) and 50% ($d = 0.498$, $p = 0.041$) immunoexpression cutoff values.

Although no statistical association was found between *PAX2* mRNA expression and ch10/*PAX2* copy number ($p = 0.919$), a positive trend was observed between these two parameters (Figure 24).

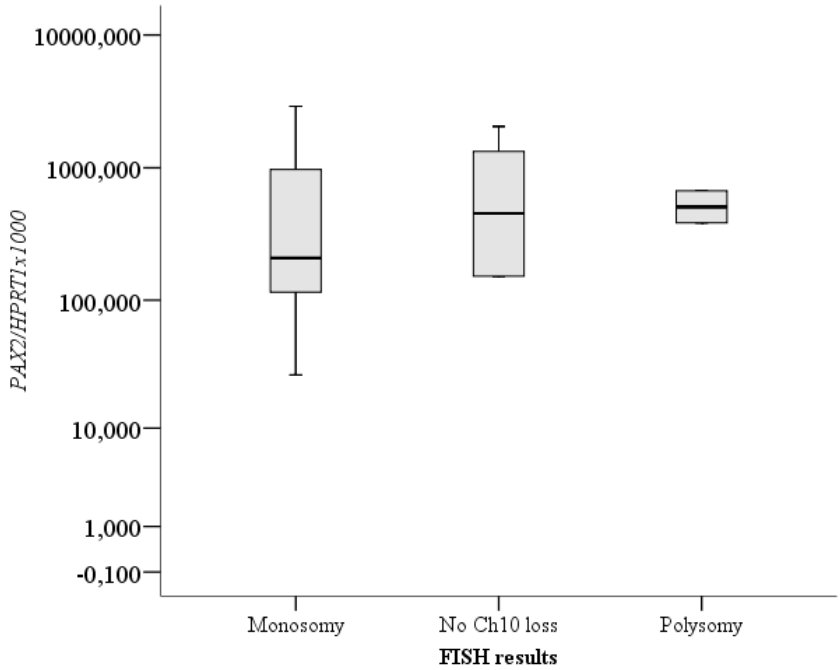

Figure 24: Boxplot of the *PAX2* mRNA expression levels (Log10 transformed) distribution according to the FISH results (n = 26).

DISCUSSION

PAX2 is an important transcription factor intensely expressed during kidney development (Chi and Epstein, 2002), which is downregulated in the latter phases of differentiation in most of the kidney structures (Dressler and Woolf, 1999). In the mature kidney, *PAX2* expression is restricted to a few structures, namely the collecting ducts and the distal tubules, where is responsible for promoting osmotic tolerance and protecting cells from apoptosis due to high sodium chloride and urea exposure (Cai *et al.*, 2005). The mechanism by which *PAX2* silencing occurs at the end of the kidney development is still controversial as some authors reported that *PAX2* promoter methylation was responsible for this downregulation (Metsuyanim *et al.*, 2008), whereas others suggested *WT1* mediated repression (Ryan *et al.*, 1995). Moreover, *PAX2* has been reported to function as an oncogene, conferring proliferative and apoptosis inhibitory characteristics to cells in several tumor models (Robson *et al.*, 2006), including renal cell tumors (Gnarra and Dressler, 1995). Finally, diffuse protein expression of PAX2 has been reported to be frequent in three of the most prevalent RCT subtypes - ccRCC, pRCC and oncocytoma - but not in chrRCC, suggesting its use for differential diagnosis in difficult cases (Mazal *et al.*, 2005; Memeo *et al.*, 2007; Gupta *et al.*, 2009).

In this study, immunohistochemical analysis of PAX2 expression disclosed significant differences among the four major subtypes of RCT. ccRCC and oncocytoma showed the highest frequency of positive cases (immunoexpression > 10% of tumor cells), whereas chrRCC showed the opposite trend. These results are in general agreement with previously published reports (Mazal *et al.*, 2005; Memeo *et al.*, 2007; Gupta *et al.*, 2009), although some differences were apparent mainly in the frequency of positive cases among chrRCC (33.3%). Because the same cutoff value was used, it is likely that methodological differences underlie these discrepant results. Indeed, we used a monoclonal antibody (which tends to be more specific), in a 1/3000 dilution, whereas all the aforementioned studies used polyclonal antibodies in 1/50 and 1/100 dilutions (Mazal *et al.*, 2005; Memeo *et al.*, 2007; Gupta *et al.*, 2009). Thus, the higher frequency of PAX2 immunoreactivity in chrRCC found in our study is not due neither to lack of antibody specificity nor to excessive concentration.

Since chrRCC (a malignant tumor) and oncocytoma (a benign tumor) may be difficult to discriminate morphologically, although they are distinct entities with different

prognosis and clinical behavior, we also aimed to confirm the potential of *PAX2* as a differential biomarker in the distinction between these two tumor subtypes. We thus determined the validity estimates using the 10% or the 50% and compared with previously published data (Mazal *et al.*, 2005; Memeo *et al.*, 2007; Gupta *et al.*, 2009). Our results follow the same trend of those studies, i.e., the 10% cutoff value offers the highest specificity, whereas, as expected, the 50% cutoff value displays the highest sensitivity. The more discrepant values are those of Mazal and co-workers as they only reported PAX2 positivity in 14% of oncocytomas, against 87 to 100% of positivity in our study and those of Memeo *et al*. and Gupta *et al*. (Mazal *et al.*, 2005; Memeo *et al.*, 2007; Gupta *et al.*, 2009). Moreover, the validity estimates obtained using a polyclonal antibody (Mazal *et al.*, 2005; Memeo *et al.*, 2007; Gupta *et al.*, 2009) are superior to those of our study, in which a monoclonal antibody was used, suggesting the use of a polyclonal antibody for the purpose of ancillary tool for histopathological diagnosis.

Interestingly, no significant differences in PAX2 immunoreactivity were found between type 1 and type 2 pRCC, corroborating the findings of Mazal *et al.* (Mazal *et al.*, 2005), notwithstanding the methodological differences. Although pRCC types 1 and 2 have been increasingly recognized as distinct subtypes, they are indistinguishable concerning PAX2 protein expression.

In line with the observations of PAX2 protein expression, *PAX2* mRNA expression also disclosed significant differences among the four RCT subtypes. However, the highest levels were observed in pRCC and ccRCC, whereas oncocytomas showed intermediate levels, and chrRCCs displayed the lowest levels of *PAX2* mRNA. Importantly, associations between PAX2 mRNA levels and protein immunoexpression were also apparent, using both immunohistochemical cutoff values, implying that PAX2 transcription and translation are correlated, although this might not be linear. The differences in PAX2 expression between pRCC and ccRCC on the one hand, and chrRCC and oncocytoma, on the other, may be related with the site of origin of each tumor type and may, thus, reflect distinct carcinogenic pathways. Indeed, whereas the former derive from proximal tubule cells, the latter originate from cortical collecting duct cells (Bodmer *et al.*, 2002). This is a somewhat unexpected finding because in normal renal tissue PAX2 expression is restricted to the distal portion of the nephron. Taken together, these findings suggest that PAX2 is overexpressed in pRCC and ccRCC, whereas in chrRCC it is underexpressed, when compared to their normal cell counterparts. Hypothetically, oncocytomas retain the normal

PAX2 expression patterns. This model is in accordance with the putative proto-oncogenic function of the *PAX2* gene (Robson *et al.*, 2006), as pRCC and ccRCC are malignant neoplasms and oncocytoma is a benign tumor. Therefore, the loss of PAX2 expression in chrRCC might be interpreted as a bystander alteration and it is tempting to speculate whether this might contribute the less aggressive clinical behavior of chrRCC compared to pRCC and ccRCC.

Correlation analyses revealed similar trends in *PAX2* expression at the protein or transcript levels and tumor grade, disclosing significant inverse correlations. Although these findings were somewhat unpredicted owing to the role ascribed to PAX2 as a transcription factor, our results are in agreement with those of Mazal *et al.,* who also reported a decrease or lack of PAX2 immunoexpression with increasing Fuhrman grade (Mazal *et al.*, 2005), and of Luu et al., although a different grading system was used and only ccRCC were analyzed (Luu *et al.*, 2009). Concerning pathological tumor stage, however, only PAX2 immunoexpression showed a significant inverse correlation, whereas the same trend was not apparent at the mRNA level. The reason for this discrepancy is not immediately apparent and may derive from the higher heterogeneity of the staging system compared to the more homogeneous nuclear grading system.

Another main objective of this study was to investigate the mechanism underlying the differential expression of *PAX2* among RCT subtypes. Two possibilities for *PAX2* gene downregulation were hypothesized: *PAX2* promoter methylation and/or deletion. The former possibility was based on the existence of a CpG island in the promoter region and the putative role of promoter methylation in PAX2 gene silencing at the final stages of kidney development (Metsuyanim *et al.*, 2008). The latter hypothesis stemmed from the observation that loss of chromosome 10 (to which *PAX2* is mapped) is a frequent event in chrRCC (Mazal *et al.*, 2005; Memeo *et al.*, 2007; Gupta *et al.*, 2009).

To test the *PAX2* promoter methylation hypothesis, methylation-specific PCR was performed not only in chrRCC but also in the remainder RCT subtypes and normal kidney tissue samples, using two different sets of primers that anneal to two adjacent regions in the promoter (Wu *et al.*, 2005; Metsuyanim *et al.*, 2008). These regions have been previously reported to be involved in *PAX2* gene transcription regulation. Strikingly, no methylation was detected in those two regions in any of the analyzed RCT samples, including chrRCC, nor in normal kidney tissues. Furthermore, no methylation was found, either, in normal endometrium (five random samples), which was previously reported to

harbor PAX2 promoter methylation using one of the primers sets (Wu *et al.*, 2005; Metsuyanim *et al.*, 2008). In addition, we tested for methylation using the other set of primers and the result was negative. Importantly, we demonstrated PAX2 protein expression in endometrial glands [which were negative according to Wu and co-workers (Wu *et al.*, 2005; Metsuyanim *et al.*, 2008)], thus validating the aforementioned methylation analysis of the *PAX2* promoter. Moreover, our results are in accordance with those of Luu *et al.* which also did not find *PAX2* promoter methylation in ccRCC or in normal kidney tissues (Luu *et al.*, 2009).

To investigate the chromosome 10 loss hypothesis, FISH analysis using specific probes for chromosome 10 and for the *PAX2* gene was performed in all cases of chrRCC included in this study. As expected, the vast majority of chrRCC cases displayed chromosome 10 monosomy, which is in accordance with the results reported by Brunelli and colleagues (Brunelli *et al.*, 2005), and no case of specific *PAX2* locus deletion was observed. These findings might explain the lower *PAX2* mRNA levels and protein expression globally observed in this tumor subtype. Remarkably, a significant association with the immunoexpression findings was apparent, indicating that chromosome 10 loss is the most likely mechanism underlying *PAX2* loss of expression. This hypothesis is further supported by the fact that cases with no copy number change or with polysomy showed higher frequency of PAX2 immunoexpression. Indeed, this trend was confirmed by the Somers'd test. Interestingly, the highest correlation value was found for the 10% immunoexpression cutoff, probably because a similar cutoff was applied to FISH analysis. Unexpectedly, no statistically significant differences were found for *PAX2* mRNA levels according to ch10/*PAX2* copy number findings, although a slight trend for increased mRNA levels in cases without ch10 monosomy was suggested. Because we previously found a significant association between PAX2 protein expression and transcript levels, this result is probably due to the limited number of cases analyzed.

This is the first study reporting FISH findings for *PAX2* gene in RCTs, to the best of our knowledge. In fact, *PAX2* locus specific deletion was not observed in any of the analyzed chrRCC samples. Therefore, we may conclude that this is not the mechanism underlying the lower *PAX2* mRNA and protein expression in the cases not showing chromosome 10 monosomy. Therefore, other yet unknown genetic or epigenetic mechanisms might justify the expression results in this small subset cases. Moreover, it is tempting to speculate whether *PAX2* gene amplification might be responsible for PAX2

overexpression in ccRCC, pRCC and oncocytomas since no ch10 copy number changes have been reported in these RCT subtypes.

CONCLUSIONS

Although PAX2 immunoexpression results diverge slightly between our study and those previously reported, our findings confirm that it still might be useful as an important ancillary tool in the distinction between the two morphologically similar entities, chrRCC and renal oncocytoma.

Our study was the first to determine the *PAX2* mRNA expression levels for the four most representative RCT subtypes, and to associate them with the respective protein expression levels. PAX2 expression was variable among the different histological subtypes, and the lowest expression, both for mRNA levels and protein, was found in the chrRCC subtype.

Importantly, our results also indicate that *PAX2* promoter methylation is not implicated in gene silencing in chrRCC or in normal kidney. Instead, the frequent chromosome 10 loss observed in chrRCC samples, and the significant correlation with PAX2 immunoexpression categories, indicate that this genetic alteration is the major cause for *PAX2* underexpression in this tumor subtype. Nonetheless, additional studies are required to accurately determine additional genetic/epigenetic regulation mechanisms underlying *PAX2* differential expression in other renal cell tumors.

ONGOING ASSAYS

This study will be completed with subsequent analysis which will further elucidate the mechanism underlying *PAX2* gene differential expression in these four major RCT subtypes.

Presently, we are performing FISH analysis on the remaining RCT subtypes used in this study. This analysis might determine whether PAX2 amplification is the genetic mechanism responsible for its overexpression in ccRCC and pRCC.

Furthermore, we aim at sequencing (bisulfite sequencing) the entire CpG island of the *PAX2* promoter region to assess if *PAX2* promoter methylation may occur in other regions besides the ones assessed in this study by reference to previously published reports.

REFERENCES

Algaba, F. 2010. Rereading the renal cell tumors. International Journal of Surgical Pathology 18 (3): 94-97.

Anglada Curado, F. J., Campos Hernandez, P., Prieto Castro, R., Carazo Carazo, J. L., Regueiro Lopez, J. C., Vela Jimenez, F. and Requena Tapia, M. J. 2009. New epidemiologic patterns and risk factors in renal cancer. Actas Urológicas Españolas 33 (5): 459-467.

Antequera, F. and Bird, A. 1993. Number of CpG islands and genes in human and mouse. Proceedings of the National Academy of Sciences 90 (24): 11995-11999.

Attwood, J. T., Yung, R. L. and Richardson, B. C. 2002. DNA methylation and the regulation of gene transcription. Cellular and Molecular Life Sciences 59 (2): 241-257.

Baldewijns, M. M., van Vlodrop, I. J., Schouten, L. J., Soetekouw, P. M., de Bruine, A. P. and van Engeland, M. 2008. Genetics and epigenetics of renal cell cancer. Biochimica et Biophysica Acta 1785 (2): 133-155.

Bennett, L. B., Schnabel, J. L., Kelchen, J. M., Taylor, K. H., Guo, J., Arthur, G. L., Papageorgio, C. N., Shi, H. and Caldwell, C. W. 2009. DNA hypermethylation accompanied by transcriptional repression in follicular lymphoma. Genes Chromosomes Cancer 48 (9): 828-841.

Bodmer, D., van den Hurk, W., van Groningen, J. J., Eleveld, M. J., Martens, G. J., Weterman, M. A. and van Kessel, A. G. 2002. Understanding familial and non-familial renal cell cancer. Human Molecular Genetics 11 (20): 2489-2498.

Bollati, V. and Baccarelli, A. 2010. Environmental epigenetics. Heredity 105 (1): 105-112.

Bose, S. K., Gibson, W., Bullard, R. S. and Donald, C. D. 2009. PAX2 oncogene negatively regulates the expression of the host defense peptide human beta defensin-1 in prostate cancer. Molecular Immunology 46 (6): 1140-1148.

Brophy, P. D., Ostrom, L., Lang, K. M. and Dressler, G. R. 2001. Regulation of ureteric bud outgrowth by Pax2-dependent activation of the glial derived neurotrophic factor gene. Development 128 (23): 4747-4756.

Brunelli, M., Eble, J. N., Zhang, S., Martignoni, G., Delahunt, B. and Cheng, L. 2005. Eosinophilic and classic chromophobe renal cell carcinomas have similar frequent losses of multiple chromosomes from among chromosomes 1, 2, 6, 10, and 17, and this pattern of genetic abnormality is not present in renal oncocytoma. Modern Pathology 18 (2): 161-169.

Buttiglieri, S., Deregibus, M. C., Bravo, S., Cassoni, P., Chiarle, R., Bussolati, B. and Camussi, G. 2004. Role of Pax2 in apoptosis resistance and proinvasive phenotype of Kaposi's sarcoma cells. Journal of Biological Chemistry 279 (6): 4136-4143.

Cai, Q., Dmitrieva, N. I., Ferraris, J. D., Brooks, H. L., van Balkom, B. W. and Burg, M. 2005. Pax2 expression occurs in renal medullary epithelial cells in vivo and in cell culture, is osmoregulated, and promotes osmotic tolerance. Proceedings of the National Academy of Sciences 102 (2): 503-508.

Calvo, S., Collins, H., Selmer, S. and Snyder, M. 2010. Chromosome 10. Version 29 March 2010. http://ghr.nlm.nih.gov/chromosome=10#ideogram in Genetics Home Reference, http://ghr.nlm.nih.gov/.

Chi, N. and Epstein, J. A. 2002. Getting your Pax straight: Pax proteins in development and disease. Trends in Genetics 18 (1): 41-47.

Cho, M., Grabmaier, K., Kitahori, Y., Hiasa, Y., Nakagawa, Y., Uemura, H., Hirao, Y., Ohnishi, T., Yoshikawa, K. and Ooesterwijk, E. 2000. Activation of the MN/CA9 gene is associated with hypomethylation in human renal cell carcinoma cell lines. Molecular Carcinogenesis 27 (3): 184-189.

Chow, W. H., Devesa, S. S., Warren, J. L. and Fraumeni, J. F., Jr. 1999. Rising incidence of renal cell cancer in the United States. The Journal of the American Medical Association 281 (17): 1628-1631.

Chow, W. H., Dong, L. M. and Devesa, S. S. 2010. Epidemiology and risk factors for kidney cancer. Nature Reviews Urology 7 (5): 245-257.

Costa, V. L., Henrique, R. and Jeronimo, C. 2007a. Epigenetic markers for molecular detection of prostate cancer. Disease Markers 23 (1-2): 31-41.

Costa, V. L., Henrique, R., Ribeiro, F. R., Pinto, M., Oliveira, J., Lobo, F., Teixeira, M. R. and Jeronimo, C. 2007b. Quantitative promoter methylation analysis of multiple cancer-related genes in renal cell tumors. BMC Cancer 7 133.

Dressler, G. R. 2008. Epigenetics, development, and the kidney. Journal of the American Society of Nephrology 19 (11): 2060-2067.

Dressler, G. R., Deutsch, U., Chowdhury, K., Nornes, H. O. and Gruss, P. 1990. Pax2, a new murine paired-box-containing gene and its expression in the developing excretory system. Development 109 (4): 787-795.

Dressler, G. R. and Woolf, A. S. 1999. Pax2 in development and renal disease. International Journal of Developmental Biology 43 (5): 463-468.

Dziarmaga, A., Eccles, M. and Goodyer, P. 2006a. Suppression of ureteric bud apoptosis rescues nephron endowment and adult renal function in Pax2 mutant mice. Journal of the American Society of Nephrology 17 (6): 1568-1575.

Dziarmaga, A., Hueber, P. A., Iglesias, D., Hache, N., Jeffs, A., Gendron, N., Mackenzie, A., Eccles, M. and Goodyer, P. 2006b. Neuronal apoptosis inhibitory protein is expressed in developing kidney and is regulated by PAX2. American Journal of Physiology - Renal Physiology 291 (4): 913-920.

Eberhard, D., Jimenez, G., Heavey, B. and Busslinger, M. 2000. Transcriptional repression by Pax5 (BSAP) through interaction with corepressors of the Groucho family. EMBO Journal 19 (10): 2292-2303.

Eble, J. N., Sauter, G., Epstein, J. I. and Sesterhenn, I. A. 2004. Pathology and Genetics of Tumours of the Urinary System and Male Genital Organs. IARC*Press*, Lyon.

Eccles, M. R., Wallis, L. J., Fidler, A. E., Spurr, N. K., Goodfellow, P. J. and Reeve, A. E. 1992. Expression of the PAX2 gene in human fetal kidney and Wilms' tumor. Cell Growth and Differentiation 3 (5): 279-289.

Edge, S. B., Byrd, D. R., Compton, C. C., Fritz, A. G., Greene, F. L. and Trotti, A. 2010. Chapter 43 - Kidney. *In* AJCC Cancer Staging Manual (Edge, S. B., Byrd, D. R., Compton, C. C., Fritz, A. G., Greene, F. L. and Trotti, A. eds.), pp. 479-489, Springer-Verlag, New York.

Ehrlich, M. 2009. DNA hypomethylation in cancer cells. Epigenomics 1 (2): 239-259.

Esteller, M. 2007. Cancer epigenomics: DNA methylomes and histone-modification maps. Nature Reviews Genetics 8 (4): 286-298.

Esteller, M. 2008. Epigenetics in cancer. New England Journal of Medicine 358 (11): 1148-1159.

Ferlay, J., Parkin, D. M. and Steliarova-Foucher, E. 2010a. Estimates of cancer incidence and mortality in Europe in 2008. European Journal of Cancer 46 (4): 765-781.

Ferlay, J., Shin, H. R., Bray, F., Forman, D., Mathers, C. and Parkin, D. M. 2010b. GLOBOCAN 2008: Cancer Incidence and Mortality Worldwide. Version 1.0, April 2010. http://globocan.iarc.fr/map.asp?selection=9200&title=Kidney&sex=9200&type=9200&statistic=9202&map=9205&window=9201&size=9201&colour=9201&scale=9200&submit=%A9200Execute%A9200 in The GLOBOCAN project, http://globocan.iarc.fr/.

Fleming, S. 2000. Classification of renal epithelial neoplasms. Current Diagnostic Pathology 6: 38-44.

Fletcher, J., Hu, M., Berman, Y., Collins, F., Grigg, J., McIver, M., Juppner, H. and Alexander, S. I. 2005. Multicystic dysplastic kidney and variable phenotype in a family with a novel deletion mutation of PAX2. Journal of the Americam Society of Nephrology 16 (9): 2754-2761.

Franklin, T. B. and Mansuy, I. M. 2009. Epigenetic inheritance in mammals: Evidence for the impact of adverse environmental effects. Neurobiology of Disease 39 (1): 61 - 65.

Fuhrman, S. A., Lasky, L. C. and Limas, C. 1982. Prognostic significance of morphologic parameters in renal cell carcinoma. The American Journal of Surgical Pathology 6 (7): 655-663.

Gibney, E. R. and Nolan, C. M. 2010. Epigenetics and gene expression. Heredity 105 (1): 4-13.

Gilbert, S. F. 2003. Developmental Biology. 7th Edition. Sinauer Associates, Inc., Sunderland, Massachusetts.

Gnarra, J. R. and Dressler, G. R. 1995. Expression of Pax-2 in human renal cell carcinoma and growth inhibition by antisense oligonucleotides. Cancer Research 55 (18): 4092-4098.

Gupta, R., Balzer, B., Picken, M., Osunkoya, A. O., Shet, T., Alsabeh, R., Luthringer, D., Paner, G. P. and Amin, M. B. 2009. Diagnostic implications of transcription factor Pax 2 protein and transmembrane enzyme complex carbonic anhydrase IX immunoreactivity in adult renal epithelial neoplasms. American Journal of Surgical Pathology 33 (2): 241-247.

Handel, A. E., Ebers, G. C. and Ramagopalan, S. V. 2010. Epigenetics: molecular mechanisms and implications for disease. Trends in Molecular Medicine 16 (1): 7-16.

Hellwinkel, O. J., Kedia, M., Isbarn, H., Budaus, L. and Friedrich, M. G. 2008. Methylation of the TPEF- and PAX6-promoters is increased in early bladder cancer and in normal mucosa adjacent to pTa tumours. British Journal of Urology International 101 (6): 753-757.

Herman, J. G., Latif, F., Weng, Y., Lerman, M. I., Zbar, B., Liu, S., Samid, D., Duan, D. S., Gnarra, J. R., Linehan, W. M. and et al. 1994. Silencing of the VHL tumor-suppressor gene by DNA methylation in renal carcinoma. Proceedings of the National Academy of Sciences 91 (21): 9700-9704.

Hueber, P. A., Waters, P., Clark, P., Eccles, M. and Goodyer, P. 2006. PAX2 inactivation enhances cisplatin-induced apoptosis in renal carcinoma cells. Kidney International 69 (7): 1139-1145.

Jemal, A., Siegel, R., Xu, J. and Ward, E. 2010. Cancer Statistics, 2010. CA Cancer Journal for Clinicians

Jeronimo, C., Usadel, H., Henrique, R., Oliveira, J., Lopes, C., Nelson, W. G. and Sidransky, D. 2001. Quantitation of GSTP1 methylation in non-neoplastic prostatic tissue and organ-confined prostate adenocarcinoma. Journal of the National Cancer Institute 93 (22): 1747-1752.

Jones, P. A. and Baylin, S. B. 2002. The fundamental role of epigenetic events in cancer. Nature Reviews Genetics 3 (6): 415-428.

Jones, P. A. and Baylin, S. B. 2007. The epigenomics of cancer. Cell 128 (4): 683-692.

Kjeldsen, E. and Kølvraa, S. 2002. FISH Techniques, FISH probes and their applications in Medicine and Biology - an Overview. *In* FISH Technology (Rautenstrauss, B. and Liehr, T. eds.), pp. 3-50, Springer-Verlag, Berlin.

Kovacs, G., Akhtar, M., Beckwith, B. J., Bugert, P., Cooper, C. S., Delahunt, B., Eble, J. N., Fleming, S., Ljungberg, B., Medeiros, L. J., Moch, H., Reuter, V. E., Ritz, E., Roos, G., Schmidt, D., Srigley, J. R., Storkel, S., van den Berg, E. and Zbar, B. 1997. The Heidelberg classification of renal cell tumours. The Journal of Pathology 183 (2): 131-133.

Lechner, M. S. and Dressler, G. R. 1996. Mapping of Pax-2 transcription activation domains. Journal of Biological Chemistry 271 (35): 21088-21093.

Lemley, K. V. and Kriz, W. 1991. Anatomy of the renal interstitium. Kidney International 39 (3): 370-381.

Lindblad, P. 2004. Epidemiology of renal cell carcinoma. Scandinavian Journal of Surgery 93 (2): 88-96.

Ljungberg, B., Cowan, N. C., Hanbury, D. C., Hora, M., Kuczyk, M. A., Merseburger, A. S., Mulders, P. F. A., Patard, J. J. and Sinescu, I. C. 2010. EAU Guidelines on Renal Cell Carcinoma: The 2010 Update. European urology 58 (3): 29-38.

Lopez-Beltran, A., Carrasco, J. C., Cheng, L., Scarpelli, M., Kirkali, Z. and Montironi, R. 2009. 2009 update on the classification of renal epithelial tumors in adults. International Journal of Urology 16 (5): 432-443.

Lopez-Serra, L. and Esteller, M. 2008. Proteins that bind methylated DNA and human cancer: reading the wrong words. British Journal of Cancer 98 (12): 1881-1885.

Lowrance, W. T., Thompson, R. H., Yee, D. S., Kaag, M., Donat, S. M. and Russo, P. 2010. Obesity is associated with a higher risk of clear-cell renal cell carcinoma than with other histologies. British Journal of Urology International 105 (1): 16-20.

Luu, V. D., Boysen, G., Struckmann, K., Casagrande, S., von Teichman, A., Wild, P. J., Sulser, T., Schraml, P. and Moch, H. 2009. Loss of VHL and hypoxia provokes PAX2 up-regulation in clear cell renal cell carcinoma. Clinical Cancer Research 15 (10): 3297-3304.

Maeshima, A., Maeshima, K., Nojima, Y. and Kojima, I. 2002. Involvement of Pax-2 in the action of activin A on tubular cell regeneration. Journal of the American Society of Nephrology 13 (12): 2850-2859.

Maulbecker, C. C. and Gruss, P. 1993. The oncogenic potential of Pax genes. EMBO Journal 12 (6): 2361-2367.

Maxwell, P. H., Wiesener, M. S., Chang, G. W., Clifford, S. C., Vaux, E. C., Cockman, M. E., Wykoff, C. C., Pugh, C. W., Maher, E. R. and Ratcliffe, P. J. 1999. The tumour suppressor protein VHL targets hypoxia-inducible factors for oxygen-dependent proteolysis. Nature 399 (6733): 271-275.

Mazal, P. R., Stichenwirth, M., Koller, A., Blach, S., Haitel, A. and Susani, M. 2005. Expression of aquaporins and PAX-2 compared to CD10 and cytokeratin 7 in renal neoplasms: a tissue microarray study. Modern Pathology 18 (4): 535-540.

McConnell, M. J., Cunliffe, H. E., Chua, L. J., Ward, T. A. and Eccles, M. R. 1997. Differential regulation of the human Wilms tumour suppressor gene (WT1) promoter by two isoforms of PAX2. Oncogene 14 (22): 2689-2700.

Memeo, L., Jhang, J., Assaad, A. M., McKiernan, J. M., Murty, V. V., Hibshoosh, H., Tong, G. X. and Mansukhani, M. M. 2007. Immunohistochemical analysis for cytokeratin 7, KIT, and PAX2: value in the differential diagnosis of chromophobe cell carcinoma. American Journal of Clinical Pathology 127 (2): 225-229.

Metsuyanim, S., Pode-Shakked, N., Schmidt-Ott, K. M., Keshet, G., Rechavi, G., Blumental, D. and Dekel, B. 2008. Accumulation of malignant renal stem cells is associated with epigenetic changes in normal renal progenitor genes. Stem Cells 26 (7): 1808-1817.

Morris, M. R., Gentle, D., Abdulrahman, M., Clarke, N., Brown, M., Kishida, T., Yao, M., Teh, B. T., Latif, F. and Maher, E. R. 2008. Functional epigenomics approach to identify methylated candidate tumour suppressor genes in renal cell carcinoma. British Journal of Cancer 98 (2): 496-501.

Mulero-Navarro, S., Esteller, M. 2008. Epigenetic biomarkers for human cancer: the time is now. Critical Reviews in Oncology/Hematology 68 (1): 1-11.

Muratovska, A., Zhou, C., He, S., Goodyer, P. and Eccles, M. R. 2003. Paired-Box genes are frequently expressed in cancer and often required for cancer cell survival. Oncogene 22 (39): 7989-7997.

Muscat, J. E. 2000. The epidemiology of Renal Cell Carcinoma. *In* Renal Cell Carcinoma, Molecular Biology, Immunology and Clinical Management (Bukowski, R. M., Novick, A.C. eds.), pp. 3-13, Humana Press, Totowa, New Jersey.

NCBI. 2010. PAX2 paired box 2 [Homo sapiens]. Version 29 March 2010. http://www.ncbi.nlm.nih.gov/gene/5076?ordinalpos=5076&itool=EntrezSystem5072.PEntrez.Gene.Gene_ResultsPanel.Gene_RVDocSum#geneReference in National Center for Biotechnology Information, http://www.ncbi.nlm.nih.gov.

Nguyen, C. T. and Campbell, S. C. 2006. Staging of renal cell carcinoma: past, present, and future. Clinical Genitourinary Cancer 5 (3): 190-197.

Palmisano, W. A., Crume, K. P., Grimes, M. J., Winters, S. A., Toyota, M., Esteller, M., Joste, N., Baylin, S. B. and Belinsky, S. A. 2003. Aberrant promoter methylation of the transcription factor genes PAX5 alpha and beta in human cancers. Cancer Research 63 (15): 4620-4625.

Pascual, D. and Borque, A. 2008. Epidemiology of kidney cancer. Advances in Urology, Article ID: 782381

Patel, S. R., Kim, D., Levitan, I. and Dressler, G. R. 2007. The BRCT-domain containing protein PTIP links PAX2 to a histone H3, lysine 4 methyltransferase complex. Developmental Cell 13 (4): 580-592.

Pearson, H. and Stirling, D. 2003. DNA extraction from tissue. Methods in Mollecular Biology 226: 33-34.

Robson, E. J., He, S. J. and Eccles, M. R. 2006. A PANorama of PAX genes in cancer and development. Nature Reviews Cancer 6 (1): 52-62.

Rosner, I., Bratslavsky, G., Pinto, P. A. and Linehan, W. M. 2009. The clinical implications of the genetics of renal cell carcinoma. Urologic Oncology 27 (2): 131-136.

Ryan, G., Steele-Perkins, V., Morris, J. F., Rauscher, F. J., 3rd and Dressler, G. R. 1995. Repression of Pax-2 by WT1 during normal kidney development. Development 121 (3): 867-875.

Sadler, T. W. 2004. Langman's Medical Embryology. 9th Edition. Lippincott Williams and Wilkins, Philadelphia.

Saladin, K. 2001. Anatomy and Physiology: The Unity of Form and Function. 2nd Edition. McGraw Hill, Boston.

Sanyanusin, P., Norrish, J. H., Ward, T. A., Nebel, A., McNoe, L. A. and Eccles, M. R. 1996. Genomic structure of the human PAX2 gene. Genomics 35 (1): 258-261.

Scarano, M. I., Strazzullo, M., Matarazzo, M. R. and D'Esposito, M. 2005. DNA methylation 40 years later: Its role in human health and disease. Journal of Cellular Physiology 204 (1): 21-35.

Schafer, B. W. 1998. Emerging roles for PAX transcription factors in cancer biology. General Physiology and Biophysics 17 (3): 211-224.

Schmidt, L., Duh, F. M., Chen, F., Kishida, T., Glenn, G., Choyke, P., Scherer, S. W., Zhuang, Z., Lubensky, I., Dean, M., Allikmets, R., Chidambaram, A., Bergerheim, U. R., Feltis, J. T., Casadevall, C., Zamarron, A., Bernues, M., Richard, S., Lips, C. J., Walther, M. M., Tsui, L. C., Geil, L., Orcutt, M. L., Stackhouse, T., Lipan, J., Slife, L., Brauch, H., Decker, J., Niehans, G., Hughson, M. D., Moch, H., Storkel, S., Lerman, M. I., Linehan, W. M. and Zbar, B. 1997. Germline and somatic mutations in the tyrosine kinase domain of the MET proto-oncogene in papillary renal carcinomas. Nature Genetics 16 (1): 68-73.

Schwarzacher, T. and Heslop-Harrison, P. 2000. Practical *in situ* Hybridization. BIOS Scientific Publishers, Oxford, UK.

Stuart, E. T. and Gruss, P. 1996. PAX: developmental control genes in cell growth and differentiation. Cell Growth and Differentiation 7 (3): 405-412.

Teyssier, J. R., Henry, I., Dozier, C., Ferre, D., Adnet, J. J. and Pluot, M. 1986. Recurrent deletion of the short arm of chromosome 3 in human renal cell carcinoma: shift of the c-raf 1 locus. Journal of the National Cancer Institute 77 (6): 1187-1195.

Thoenes, W., Storkel, S., Rumpelt, H. J., Moll, R., Baum, H. P. and Werner, S. 1988. Chromophobe cell renal carcinoma and its variants--a report on 32 cases. Journal of Pathology 155 (4): 277-287.

Torban, E., Eccles, M. R., Favor, J. and Goodyer, P. R. 2000. PAX2 suppresses apoptosis in renal collecting duct cells. American Journal of Pathology 157 (3): 833-842.

Wang, Q., Fang, W. H., Krupinski, J., Kumar, S., Slevin, M. and Kumar, P. 2008. Pax genes in embryogenesis and oncogenesis. Journal of Cellular and Molecular Medicine 12 (6A): 2281-2294.

Ward, T. A., Nebel, A., Reeve, A. E. and Eccles, M. R. 1994. Alternative messenger RNA forms and open reading frames within an additional conserved region of the human PAX-2 gene. Cell Growth and Differentiation 5 (9): 1015-1021.

Wu, H., Chen, Y., Liang, J., Shi, B., Wu, G., Zhang, Y., Wang, D., Li, R., Yi, X., Zhang, H., Sun, L. and Shang, Y. 2005. Hypomethylation-linked activation of PAX2 mediates tamoxifen-stimulated endometrial carcinogenesis. Nature 438 (7070): 981-987.